VOLUME FIVE

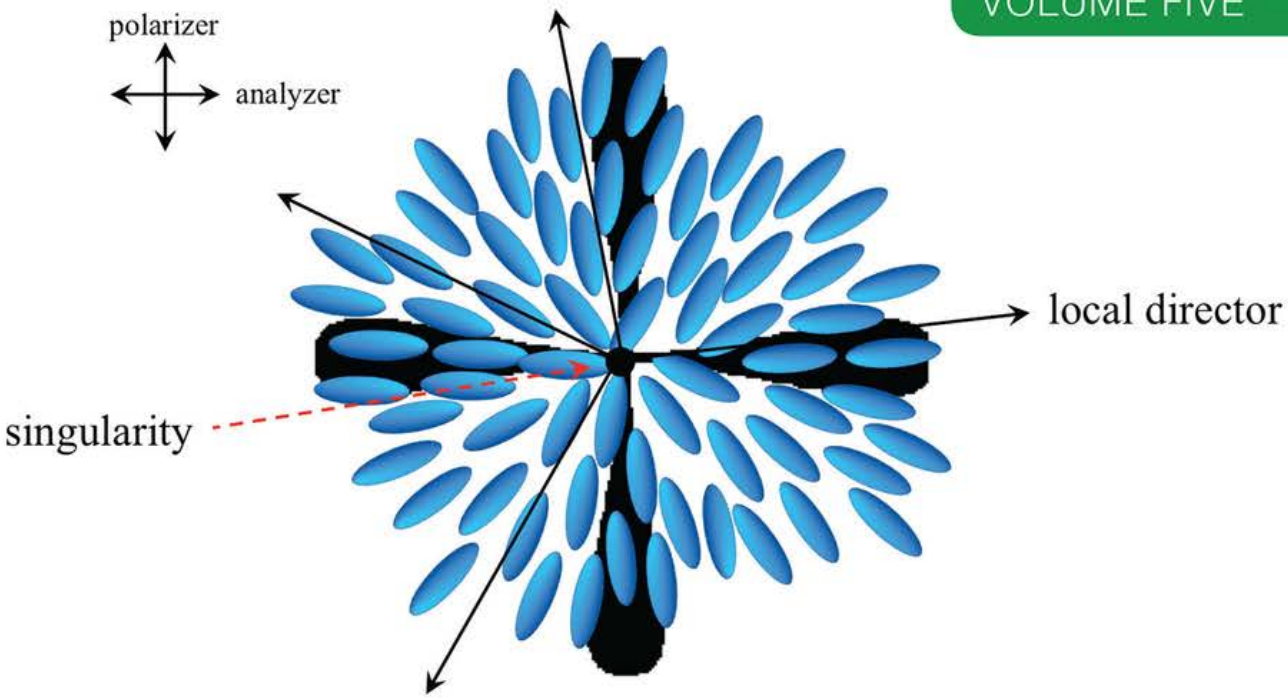

21st Century Nanoscience
A Handbook

Exotic Nanostructures and Quantum Systems

edited by
Klaus D. Sattler

CRC Press
Taylor & Francis Group

22

Nanothermodynamics: Fundamentals and Applications

Vladimir García-Morales, Javier Cervera, and José A. Manzanares
University of Valencia

22.1 Introduction

Atoms at the surface and, therefore, surface energies have a marked influence on the physical and chemical properties of nanoscale materials due to their high surface to volume ratio. These properties often obey relatively simple scaling equations involving a power-law dependence on the system size, which can be explained from the surface energy contributions to the free energy. An adequate description of these contributions is then essential to understand the thermodynamic behavior of nanoscale systems.

Hill's nanothermodynamics [Hill, 1994, Hill, 2001] is a framework to properly describe the equilibrium thermodynamics of small systems that was initially developed from the applications of statistical thermodynamics to polymers and biomacromolecules. Ralph V. Chamberlin realized that the small systems do not need to be separate entities and considered that a bulk material could be divided into small regions, so that the methods of Hill's theory could be applied. The consideration of inhomogeneous regions of unrestricted sizes in combination with relatively simple mean-field models or with Landau theory of phase transitions has resulted in significant advances in the understanding of many complex systems, including non-exponential relaxation phenomena in glasses [Chamberlin, 2015].

Tsallis' thermostatistics [Tsallis, 1988, Tsallis, 2009] is a generalization of Boltzmann–Gibbs statistical mechanics to make it valid in complex nonextensive systems, including nanosized systems and systems with correlations or long-range interactions. Tsallis' entropic index q has often been considered to be intimately related to and determined by the microscopic dynamics. Many authors have contributed to the clarification of its physical foundations [Abe and Okamoto, 2001, Tsallis, 2009, Naudts, 2011], including its connection to Hill's nanothermodynamics [García-Morales et al., 2005]. In this chapter, Tsallis' theory is briefly outlined within the more general context of superstatistics [Beck, 2002, García-Morales et al., 2011].

As the system size decreases, the fluctuations in the equilibrium thermodynamic variables become more important. Temperature fluctuations, in particular, have received much attention both from theoretical and experimental points of view, especially with the recent advances in

nanothermometry [Brites et al., 2012]. In this chapter, the equilibrium fluctuations are described within the context of Einstein's theory [Falcioni et al., 2011].

The attention to nonequilibrium thermodynamics and fluctuations can be traced back to Einstein, but the field underwent a revolution in the early 1990s [Evans et al.; 1993]. Since then, researchers have been proposing a growing number of fluctuation theorems (FTs) [Sevick et al., 2008, Evans et al., 2016] and fluctuation relations [Spinney and Ford, 2013, Ford, 2013]. In fact, any convex function defined over a trajectory may lead to functionals that satisfy an integral FT. The FTs seem at odds with the traditional nineteenth-century thermodynamics and have changed our understanding of equilibrium and nonequilibrium thermodynamics. The Evans–Searles FT [Evans and Searles, 1994, Evans et al., 2016] results in a generalization of the second law that applies to small systems, including those far from equilibrium. The Crooks FT [Crooks, 1999] provides a method of predicting equilibrium free energy differences from nonequilibrium paths that connect two equilibrium states. Undoubtedly, the FTs are essential for the application of statistical mechanics concepts to irreversible processes of nanoscale systems [Seifert, 2012].

The FTs can be derived within a framework of deterministic, time-reversible mechanics [Evans et al., 2016] and from stochastic dynamics (often with white noise and using the overdamped limit) [Kurchan, 1998,Lebowitz and Spohn, 1999,Spinney and Ford, 2013,Seifert, 2012]. In the deterministic framework, irreversibility finds its origins in nonlinear terms that provide a contraction of phase space. In the stochastic approach, irreversibility directly appears in the dynamical equation. In this chapter, only the stochastic approach is described, but applications to chemical and electrochemical systems are also explained in detail.

The lack of sound mechanical or quantum-mechanical foundations of thermodynamics has been seen as a major unsolved problem. Recently, there have been interesting attempts to rebuild thermodynamics from quantum mechanics, as the latter is the framework required in practical applications to nanoelectronic components and atom-sized or single-molecule machines [Brandao et al., 2015, Horodecki and Oppenheim, 2013]. They are, however, out of the scope of the present chapter, and the interested reader is referred to recent books [Mahler, 2015] and contributions presented at the quantum thermodynamics conferences [Castelvecchi, 2017].

22.2 Surface Thermodynamics of Nanomaterials

22.2.1 The Gibbs, Euler, and Gibbs–Duhem Equations in Surface Thermodynamics

Surface thermodynamics is a successful framework to describe the smooth size effects on the physicochemical properties. Consider an interfacial region, a few atomic diameters in thickness, that separates two homogeneous phases α and β. In this region, the densities of the extensive quantities vary smoothly with position, from their values in phase α to those in β [Inzoli et al., 2010, Li and Truhlar, 2014]. This smooth variation can be replaced by an equivalent, abrupt variation so that the methods of macroscopic thermodynamics can still be used. The interfacial region, or phase σ, is then represented by an imaginary surface, the Gibbs dividing surface. In planar geometry, the extension of the interfacial region is $-x^\alpha \le x \le x^\beta$, where x is the distance to the interface and $-x^\alpha$ and x^β are two positions inside phases α and β close to the interface. Consider an extensive quantity Y such as energy, entropy, or the amount n_i of component i. The amount of Y in the interfacial region is $\Sigma \int_{-x^\alpha}^{x^\beta} y_V(x)dx$, where Σ is the area of the interface and $y_V(x)$ is the local density of Y. In the Gibbs description, this same amount is evaluated extrapolating the densities y_V^α and y_V^β in phases α and β. The equivalence of these descriptions requires $y_V^\alpha x^\alpha \Sigma + y_V^\beta x^\beta \Sigma + Y^\sigma = \Sigma \int_{-x^\alpha}^{x^\beta} y_V(x)dx$ where Y^σ is the surface *excess* of Y, which can be positive, negative, or zero. For instance, the surface excess entropy S^σ is the contribution of the interface to the entropy of a system formed by two homogenous phases α and β and the interface σ.

The position of the Gibbs surface is chosen so that the surface excess of the amount of component 1 (e.g., the solvent) is zero $n_1^\sigma = 0$, that is, $c_1^\alpha x^\alpha + c_1^\beta x^\beta = \Sigma \int_{-x^\alpha}^{x^\beta} c_1(x)dx$. Because different components have different tendencies to accumulate in the interfacial region, the surface excesses of the other components are usually nonzero, $n_{i\neq 1}^\sigma \neq 0$ [Inzoli et al., 2010].

The area Σ describes the size of the interface, and a convenient choice of state variables is $(T, \Sigma, \mathbf{n}^\sigma)$, where $\mathbf{n}^\sigma = \{0, n_2^\sigma, \ldots, n_c^\sigma\}$. A consistent choice for phases α and β is $(T, V^\alpha, \mathbf{n}^\alpha)$ and $(T, V^\beta, \mathbf{n}^\beta)$. The Gibbs equations in the free energy representation are

$$dA^\varphi = -S^\varphi dT - p^\varphi dV^\varphi + \sum_i \mu_i dn_i^\varphi, \qquad \varphi = \alpha, \beta, \tag{22.1}$$

$$dA^\sigma = -S^\sigma dT + \gamma d\Sigma + \sum_{i\neq 1} \mu_i dn_i^\sigma, \tag{22.2}$$

where $\gamma \equiv (\partial A^\sigma/\partial\Sigma)_{T,n^\sigma}$ is the interfacial free energy. Under equilibrium conditions, the temperature T and the chemical potentials μ_i do not need phase superscripts as they take the same values in phases α, β, and σ; there are, however, generalized approaches that allow for temperature differences between the phases [Schmelzer et al., 2013].

For a bulk phase $\varphi = \alpha, \beta$, the Euler equation

$$A^\varphi = -p^\varphi V^\varphi + \sum_i \mu_i n_i^\varphi \tag{22.3}$$

is a consequence of the system extensivity. That is, if T and the concentrations $\mathbf{c}^\varphi$ are fixed, then A^φ and $\mathbf{n}^\varphi$ scale linearly with V^φ. Similarly, A^σ and $\mathbf{n}^\sigma$ scale linearly with the surface area Σ, for fixed intensive state, and the Euler equation of A^σ is

$$A^\sigma(T,\Sigma,\mathbf{n}^\sigma) = \gamma\Sigma + \sum_{i\neq 1}\mu_i n_i^\sigma. \tag{22.4}$$

Furthermore, the Euler theorem for homogeneous functions implies that the surface density of excess free energy $a^\sigma \equiv A^\sigma/\Sigma$; the chemical potentials μ_i and γ are independent of Σ. Dividing by Σ, Eq. (22.4) reduces to $a^\sigma = \gamma + \sum_{i\neq 1}\mu_i\Gamma_i^\sigma$. In one-component systems, $a^\sigma = \gamma$ justifies the name "interfacial free energy" for γ.

In the case of curved interfaces, the pressure can be different in phases α and β. According to the second law, a mechanical equilibration process in which the volumes of these phases vary at fixed $(T, V^\alpha + V^\beta, \mathbf{n})$, where $n_i = n_i^\alpha + n_i^\sigma + n_i^\beta$, ends in a state of minimum free energy $A = A^\alpha + A^\sigma + A^\beta$,

$$\left(\frac{\partial A}{\partial V^\alpha}\right)_{T,V,\mathbf{n}} = -p^\alpha + p^\beta + \gamma\left(\frac{\partial\Sigma}{\partial V^\alpha}\right)_{T,\mathbf{n}} = 0. \tag{22.5}$$

When phase α is a spherical drop of radius r, $dV^\alpha = 4\pi r^2 dr$ and $d\Sigma = 8\pi r dr = (2/r)dV^\sigma$. Then, Eq. (22.5) becomes the Young–Laplace equation

$$p^\alpha = p^\beta + \frac{2\gamma}{r}. \tag{22.6}$$

The pressure is larger there in the phase α from which the interface looks concave. The instability induced by the curvature can be illustrated considering a volume transfer between the inside of two drops of different radii. Since p^α increases when r decreases, the larger drop would grow, and the smaller one would disappear.

22.2.2 Size Effects on the Thermodynamic Properties of Monocomponent Nanosystems

In one-component systems, the distribution equilibrium condition along the saturation curve, $d\mu^\alpha = d\mu^\beta$ or $-s^\alpha dT + v^\alpha dp^\alpha = -s^\beta dT + v^\beta dp^\beta$, leads to the generalized Clausius–Clapeyron equation

$$(s^\beta - s^\alpha)dT - (v^\beta - v^\alpha)dp^\beta + 2v^\alpha d(\gamma/r) = 0, \tag{22.7}$$

where $v^\varphi \equiv V^\varphi/n^\varphi$ and $s^\varphi \equiv S^\varphi/n^\varphi$ are the molar volume and molar entropy of phase $\varphi = \alpha, \beta$. For a solid or liquid phase α in equilibrium with a vapor phase β (i.e., under saturation conditions), the chemical potential is a function of T and r, because $\mu^\alpha = \mu^\beta$ fixes the pressures $p^\beta = p_{\rm sat}^{\alpha\beta}(T,r)$ and $p^\alpha = p^\beta + 2\gamma/r$. Since $v^\beta >> v^\alpha$ and $d\mu = v^\beta dp^\beta \approx (v^\beta - v^\alpha)dp^\beta = 2v^\alpha d(\gamma/r)$ at constant T, integration with respect to $1/r$ leads to the

Gibbs–Thomson–Freundlich equation

$$\mu_{\rm sat}^{\alpha\beta}(T,r) = \mu_{\rm sat}^{\alpha\beta}(T,\infty) + \frac{2\gamma v^\alpha}{r}. \tag{22.8}$$

The interfacial system $\alpha+\sigma$ satisfies $dG^{\alpha+\sigma} + S^{\alpha+\sigma}dT - V^\alpha dp^\alpha = \mu^\alpha dn^\alpha + \gamma d\Sigma = \mu^{\alpha+\sigma}dn^\alpha$. Contrarily to $\mu^\alpha = \mu_{\rm sat}^{\alpha\beta}(T,\infty)$, $\mu^{\alpha+\sigma} = \mu^\alpha + \gamma(\partial\Sigma/\partial n^\alpha) = \mu_{\rm sat}^{\alpha\beta}(T,r)$ includes the surface free energy contribution. Note also that $G^{\alpha+\sigma} = \mu^{\alpha+\sigma}n^\alpha + \gamma\Sigma/3$.

The vapor pressure of metallic nanoparticles is notably higher than that of the bulk material [Nanda et al., 2003]. Indeed, if phase β is the vapor of a condensed phase α, then the integration of Eq. (22.7) at constant T leads to Kelvin's equation

$$\frac{p^\beta(T,r)}{p^\beta(T,\infty)} = \exp\left(\frac{2\gamma v^\alpha}{RTr}\right) \geq 1. \tag{22.9}$$

Nanoparticles can only be in equilibrium with a supersaturated vapor because they have a greater tendency to evaporate than a flat surface of the bulk material at the same T. This effect is only noticeable if the radius is not much larger than the so-called Kelvin radius (e.g., $2\gamma v^L/RT = 1.04$ nm for water at 300 K). Thus, solid–vapor and liquid–vapor saturation curves on a p–T diagram shift to higher pressures with decreasing drop size, and in the opposite direction in the case of nanobubbles. Kelvin's equation describes an unstable equilibrium as any perturbation drives the nanoparticle away from the equilibrium state. A stable distribution equilibrium is only possible at flat interfaces or in muticomponent condensed nanophases but not in single component ones.

The melting temperature $T_m(r)$ of metallic nanoparticles is lower than that of the bulk material. William Thomson (Lord Kelvin) in 1870 and J. J. Thomson in 1888 were already interested in this phenomenon, and Pawlow established the first thermodynamic relation for $T_m(r)$ in 1909. The melting point depression is observable in nanoparticles with radius r below 100 nm and is very large for radii in the nm range. For example, a Pb nanoparticle of radius 3 nm. Please note that although 1,800 is customary in conventional English, it is not correct in scientific English, as regulated by the International System of Units and the ISO 80000 standards. (about 1800 atoms) has a standard melting temperature 200 K lower than bulk Pb ($T_m^b = 600$ K) [Kofman et al., 1999].

At constant p^β, Eq. (22.7) can be integrated to give

$$\ln\frac{T(p^\beta,r)}{T(p^\beta,\infty)} = -\frac{2\gamma v^\alpha}{h^\beta - h^\alpha}\frac{1}{r}, \tag{22.10}$$

where the distribution equilibrium condition $h^\beta - h^\alpha = T(s^\beta - s^\alpha)$ has been used. When applied to the liquid–vapor equilibrium, the vaporization temperature of liquid drops decreases with decreasing size, $T_{\rm vap}(p^V,r) < T_{\rm vap}(p^V,\infty)$. When applied to the (melting) equilibrium between solid nanoparticles and their liquid phase, $h^\beta - h^\alpha = \Delta H_m^b$ is the bulk molar enthalpy of melting and $T_m(r) = T_m(p^L,r) < T_m(p^L,\infty) = T_m^b$. Spherical particles then melt at lower temperatures than the corresponding bulk phase. If we use that $\ln x \approx x-1$ when $x \approx 1$, Eq. (22.10) can be transformed to [Couchman and Jesser, 1977]

$$1 - \frac{T_m(r)}{T_m^b} = \frac{2\gamma^{SL}v^S}{\Delta H_m^b}\frac{1}{r}. \tag{22.11}$$

Most theoretical models for the dependence of the melting point on the particle size predict similar expressions [Jiang and Wen, 2011].

The $1/r$ dependence is widely accepted for metallic nanoparticles with diameters larger than a few nanometers; group IV semiconductors show a $1/r^2$ dependence and hence lower vapor pressure increase and lower melting point depressions [Farrell and Van Siclen, 2007]. For smaller diameters, $T_m(r)$ depends nonlinearly on $1/r$ [Chushak and Bartell, 2001]. The study of the melting transition of atomic clusters is necessarily more complicated not only because of experimental difficulties, but also because the very concept of melting has no meaning for atoms and molecules. Moreover, a slush phase is observed between the freezing and melting temperatures that determine the boundaries of the solid and liquid phases [Li and Truhlar, 2014].

Although phase transitions in nanosystems are always continuous, melting of Pb nanoparticles with diameter larger than 5 nm has been considered to be first-order [Kofman et al., 1999]. The order parameter in the system (density, crystallinity, etc.) evolves continuously with radial coordinate but discontinuously with temperature. The melting process is to be understood as a nucleation and growth phenomenon of the liquid on the solid. This phenomenon is favored if the liquid wets the solid, i.e., if $\Delta\gamma \equiv \gamma^{SV} - \gamma^{SL} - \gamma^{LV} > 0$ and there is a gain in energy when a solid surface layer is replaced by a liquid one [Peters et al., 1998, Shi et al., 2004]. The surface liquid layer starts with a continuous growth and suddenly invades the cluster at $T = T_m(r)$ and $r_c = r_m$. In other words, the solid core has a radius r_c which varies from the particle radius r at low temperatures to a critical value r_m when the particle melts. At this critical value of the cluster radius, both surface melting and irreversibility in freezing disappear. For nonspherical nanoparticles, the thickness δ of the liquid surface layer depends on the local curvature so that high curvature regions enhance surface melting.

The influence of curved interfaces upon the behavior of materials is manifested primarily through the shift of phase boundaries on phase diagrams derived from the altered condition of mechanical equilibrium [Defay and Prigogine, 1966, Dehoff, 2006]. For a number of substances, the stable phase at standard conditions is not that of highest density, as the latter is usually stable at higher pressures or lower temperatures. However, a metastable high-pressure phase can be formed at ambient pressure when the material size decreases to the nanoscale. For instance, in the nucleation stage of clusters from gases during chemical vapor deposition, the phase stability is quite different from that determined at ambient pressure. The high additional internal pressure associated with the interfacial free energy through Young–Laplace equation makes it possible to observe "unusual" phases [Zhang et al., 2004, Wang et al., 2004, Wang and Yang, 2005]. Thus, for instance, diamond has been found to be more stable than graphite in small nanocrystals [Yang and Li, 2008].

22.2.3 Ostwald Ripening and Digestive Ripening in Ensembles of Nanoparticles

The chemical potential $\mu^\alpha = \mu^\beta = \mu$ increases with decreasing radius r of the condensed phase α. Since the chemical potential is a measure of the escaping tendency of the component, a larger chemical potential indicates a lower stability, e.g., with respect to phase transitions. The Ostwald ripening phenomenon is a consequence of the higher chemical potential of smaller drops. When drops of different sizes coexist, the component that forms the drops transfers from the smaller ones, where its chemical potential is larger, to the larger ones, where its chemical potential is smaller. If the drops coexist with a bulk phase of the same component, they tend to disappear due to the transfer of component from the drops to the bulk phase. Interestingly, the Ostwald ripening growth mechanism can lead to size-dependent composition in the case of nanoalloys [Alloyeau et al., 2010].

While a narrow size distribution is essential for most applications, Ostwald ripening, sintering, and coalescence induce polydispersity. These processes can be limited, e.g., in colloidal-based synthesis, but most synthetic protocols have to include a digestive ripening thermochemical step in which polydisperse nanoparticles are transformed to a narrower size distribution of ligand-stabilized metallic nanoparticles [Manzanares et al., 2017]. The size distribution after the digestive ripening process is determined by the thermodynamic stability. The free energy minimization of the colloidal solution over all possible distributions determines the relation between the Gibbs free energy of a nanoparticle made of N atoms and the chemical potential of the metal atoms. Nanoparticles of different sizes have different mole fractions in solution; that is, there is a probability distribution function for the size under equilibrium conditions. The capping ligands exert a key role, with stronger binding ligands giving rise to smaller average sizes [Manzanares et al., 2017].

22.2.4 Size Effects on the Phase Diagrams of Binary Systems

Consider the formation of a saturated liquid solution by mixing a solvent (1) and a solid solute (2), both at the same temperature T and pressure p. The molar fraction at saturation $x_2^{L,\mathrm{sat}}(T,\infty)$ is a measure of its solubility. A supersaturated phase with $x_2^L > x_2^{L,\mathrm{sat}}(T,\infty)$ can be formed, at the same T and p, by cooling a liquid mixture with composition x_2^L. This liquid phase can remain metastable because the nucleation of crystallites of pure solute implies the formation of a curved solid–liquid interface with radius in the nanometer scale, and the solubility limit $x_2^{L,\mathrm{sat}}(T,\infty)$ only applies to planar interfaces.

The distribution equilibrium condition is $\mu_2^{*,S} = \mu_2^L$. Since $\mu_2^{*,S}(T,p) = \mu_2^{*,L}(T,p) - \Delta H_{m,2}(1 - T/T_{m,2})$ and $\mu_2^L(T,p,x_2^{L,\mathrm{sat}}) = \mu_2^{*,L}(T,p) + RT\ln x_2^{L,\mathrm{sat}}$ (if the solution

is considered an ideal mixture); the equilibrium requires $T < T_{m,2}$; and the solubility

$$x_2^{L,\mathrm{sat}}(T,\infty) = \exp\left[\frac{\Delta H_{m,2}}{R}\left(\frac{1}{T_{m,2}} - \frac{1}{T}\right)\right] \qquad (22.12)$$

increases with T. Equation (22.12) is valid for planar solid–liquid interfaces. Solute nanoparticles with different radii have different solubilities because of the pressure difference induced by the interfacial free energy, $p^S = p^L + 2\gamma^{SL}/r$. The solute chemical potential in the nanoparticles increases with decreasing radius $\mu_2^{*,S}(T,p^S) = \mu_2^{*,S}(T,p^L) + (p^S - p^L)v^S = \mu_2^{*,S}(T,p^L) + 2\gamma^{SL}v^S/r$, and hence the solubility increases. The condition $\mu_2^{*,S}(T,p) = \mu_2^{*,L}(T,p,x_2^{L,\mathrm{sat}})$ leads then to the Ostwald–Freundlich equation

$$\frac{x_2^{L,\mathrm{sat}}(T,r)}{x_2^{L,\mathrm{sat}}(T,\infty)} = \exp\left(\frac{2\gamma^{SL}v^S}{RTr}\right). \qquad (22.13)$$

Thus, solid nanoparticles can only be in equilibrium with a supersaturated solution [Kondepudi, 2008, Defay and Prigogine, 1966, Sugimoto and Shiba, 1999].

The liquidus curve describing the distribution equilibrium of component 2 between pure solid nanoparticles and the liquid solution in a temperature–composition diagram is

$$\ln x_2^{L,\mathrm{sat}}(T,r) = \frac{\Delta H_{m,2}}{R}\left(\frac{1}{T_{m,2}} - \frac{1}{T}\right) + \frac{2\gamma^{SL}v^S}{RTr}. \quad (22.14)$$

In general, due to the interfacial free energy contribution to the chemical potentials of the components, the equilibrium curves in the phase diagrams of binary mixtures shift significantly with the nanoscale radii of the interfaces [Park and Lee, 2008, Pohl et al., 1998, Jabbareh and Monji, 2018].

The theoretical calculation of phase diagrams of nanosystems often consider closed systems in the microcanonical ensemble [Kaszkur, 2013]. However, the different ensembles are not equivalent in the nanoscale, and the consideration of completely open nanosystems in the nanocanonical ensemble might be more realistic, as the fluctuations themselves are to govern the distribution of grain sizes [Chamberlin, 2015].

Equation (22.14) predicts that the liquidus curve shifts toward lower temperatures, and this implies that in eutectic mixtures, the eutectic temperature must decrease with decreasing nanoparticle size as observed experimentally [Chen et al., 2011]. In the case of ideal liquid mixture and solid phases which are practically pure (i.e., the case of immiscibility in solid phase), the liquidus curves are given by Eq. (22.14) and a similar one for component 1. The eutectic point belongs to both curves, and its temperature $T = T_{\mathrm{eut}}(r)$ can be determined as a function of the radius from the condition $x_1^{L,\mathrm{eut}} + x_2^{L,\mathrm{eut}} = 1$. In the case of planar interfaces ($r \to \infty$), this condition would determine the bulk eutectic temperature $T_{\mathrm{eut}}(\infty)$. A first-order series expansion of $x_1^{L,\mathrm{eut}} + x_2^{L,\mathrm{eut}} = 1$ in powers of $1/r$ gives

$$\frac{T_{\mathrm{eut}}(r)}{T_{\mathrm{eut}}(\infty)} = 1 - 2\frac{x_1^{L,\mathrm{eut}}\gamma_1^{SL}v_1^S + x_2^{L,\mathrm{eut}}\gamma_2^{SL}v_2^S}{x_1^{L,\mathrm{eut}}\Delta H_{m,1} + x_2^{L,\mathrm{eut}}\Delta H_{m,2}}\frac{1}{r}. \quad (22.15)$$

This expression is in good agreement with the measured $T_{\mathrm{eut}}(r)$ of Ag–Pb alloy nanoparticles of different sizes (Figure 22.1). More accurate descriptions might take into account deviations from ideality and the composition of the solid phases, but the basic trend of lowering $T_{\mathrm{eut}}(r)$ with a term proportional to $1/r$ would be reproduced as this is a surface-induced phenomenon.

22.2.5 Size Dependence of the Interfacial Free Energy

The surface free energy $\gamma\Sigma$ of gold nanoparticles with n atoms evaluated from MD simulations can be accurately fitted to $\gamma\Sigma = an^{2/3}$ with $a = (1.8765 \pm 0.0085)$ eV, and for large radii, it simplifies to $\gamma_\infty 4\pi r^2$ with $\gamma_\infty = 0.98$ J/m^2 (Figure 22.2). The interfacial free energy γ varies with the nanoparticle size, and decrease as well as increase with decreasing size have been observed [Manzanares et al., 2017]. For very small nanoparticles, the validity of Tolman's equation [García-Morales et al., 2011] has been questioned [Nanda et al., 2003, Lu and Jiang, 2014], but these apparently contradictory observations might simply reflect

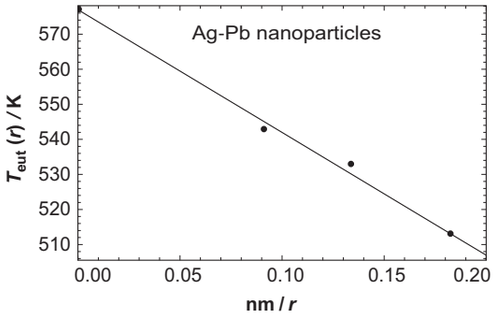

FIGURE 22.1 Measured eutectic temperatures of Ag–Pb alloy nanoparticles [Chen et al., 2011] and their comparison with the predictions by Eq. (22.15) with $\gamma_1^{SL} = \gamma_2^{SL} = 0.7$ J/m^2.

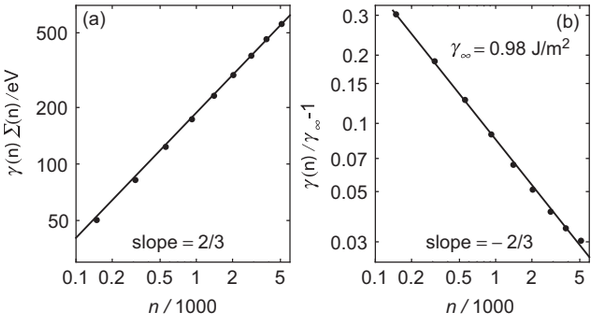

FIGURE 22.2 (a) Surface energy contribution from MD simulations [Ali et al., 2016] to the Gibbs potential of gold NPs containing n atoms. (b) Because of the increase in the fraction of edge and corner sites, $\gamma(n)$ increases with decreasing NP size [Manzanares et al., 2017]. In addition to the leading term $\propto n^{2/3}$, the surface area $\Sigma(n)$ has other size-dependent contributions, and a compensation of effects results in a reasonable accuracy of the simple expression $\gamma\Sigma = an^{2/3}$.

different conventions. When the surface atoms are compared to those in the nanoparticle core, a decrease in size reduces their energy difference. However, when the surface atoms are compared to those in bulk metal, a decrease in NP size increases their energy difference.

22.2.6 Size Effects on the Reduction Potential of Nanoparticles

Due to the interfacial free energy contribution, a metallic nanoparticle becomes less stable as its radius decreases. This also implies lower electrochemical stability. Stripping voltammetry of metallic nanoparticles on a conducting surface shows that the peak potential representing the oxidative dissolution of the metallic nanoparticle shifts negatively as r decreases. That is, the nanoparticles oxidize more easily due to the decreased stability. For the reduction of a metal cation resulting in the addition of a metal atom to the nanoparticle, the standard redox potential differs from that on a bulk metal electrode. Plieth predicted that the standard redox potential of a metal in a nanoparticle is decreased by $2\gamma v/er$, where v is the volume per atom and e is the elementary charge. Electrostatic charging effects must also be considered as they also affect the redox potential [Scanlon et al., 2015, Peljo et al., 2016, Peljo et al., 2017].

22.3 Equilibrium Nanothermodynamics

22.3.1 Hill's Subdivision Potential and the Generalized Ensemble

Compare two composite systems with the same variables (S_t, V_t, N_t) and differing in the number of subsystems (or small systems). One system has $\mathfrak{N}_1$ subsystems, each with internal energy U_1 and characterized by $S_1 = S_t/\mathfrak{N}_1$, $V_1 = V_t/\mathfrak{N}_1$ and $N_1 = N_t/\mathfrak{N}_1$. The other has $\mathfrak{N}_2$ subsystems with internal energy U_2 and variables $S_2 = S_t/\mathfrak{N}_2$, $V_2 = V_t/\mathfrak{N}_2$ and $N_2 = N_t/\mathfrak{N}_2$. In macroscopic thermodynamics, the Euler equations $U_1 = TS_1 - pV_1 + \mu N_1$ and $U_2 = TS_2 - pV_2 + \mu N_2$ imply $\mathfrak{N}_1 U_1 = \mathfrak{N}_2 U_2$, i.e., $U_{t1}(S_t, V_t, N_t, \mathfrak{N}_1) = U_{t2}(S_t, V_t, N_t, \mathfrak{N}_2)$, so that U_t is a function of (S_t, V_t, N_t) and independent of $\mathfrak{N}$. However, the Euler equation needs a correction when it is experimentally observed that $U_{t1}(S_t, V_t, N_t, \mathfrak{N}_1) \neq U_{t2}(S_t, V_t, N_t, \mathfrak{N}_2)$.

Hill's nanothermodynamics is a generalization of macroscopic thermodynamics to account for finite-size effects via the introduction of the *subdivision potential* $\mathcal{E}$. In this theory, U_t is a function of (S_t, V_t, N_t) and the number $\mathfrak{N}$ of subsystems. Therefore, the Gibbs equation of the composite system is

$$dU_t = TdS_t - pdV_t + \mu dN_t + \mathcal{E}d\mathfrak{N}, \tag{22.16}$$

where the subdivision potential is defined as

$$\mathcal{E} \equiv \left(\frac{\partial U_t}{\partial \mathfrak{N}}\right)_{S_t,V_t,N_t} \approx U_t(S_t, V_t, N_t, \mathfrak{N} + 1) - U_t(S_t, V_t, N_t, \mathfrak{N}), \tag{22.17}$$

and can be interpreted as the (positive or negative) energy required to increase in one unit the number $\mathfrak{N}$ of subdivisions of the system, while keeping constant (S_t, V_t, N_t). Thus, $(\mathcal{E}, \mathfrak{N})$ is a pair of conjugate quantities similar to (T, S_t), (p, V_t) and (μ, N_t).

Since the composite system is macroscopic and the small systems are non-interactive, U_t is a first-order homogeneous function of its extensive variables, $\mathfrak{N}$ included, and the Euler theorem implies then $U_t = TS_t - pV_t + \mu N_t + \mathcal{E}\mathfrak{N}$ and $\mathfrak{N}d\mathcal{E} = -S_t dT + V_t dp - N_t d\mu$. Division by $\mathfrak{N}$ leads to the Euler and Gibbs–Duhem equations of a small system

$$G = U - TS + pV = \mu N + \mathcal{E}, \tag{22.18}$$

$$d\mathcal{E} = -SdT + Vdp - Nd\mu. \tag{22.19}$$

Remarkably, the Gibbs equation of a small system is the same as in macroscopic thermodynamics

$$dU = TdS - pdV + \mu dN. \tag{22.20}$$

Equation (22.19) evidences that T, p, and μ can be varied independently, because the size of the small systems is an additional degree of freedom, and that the subdivision potential $\mathcal{E}$ is the thermodynamic potential whose natural variables are (T, p, μ).

The generalized, completely open, or nanocanonical ensemble [Chamberlin, 2015] considers systems with thermal, mechanical, and material interactions with its surroundings so that (T, p, μ) are environmentally-fixed variables. Equivalently, this set can be transformed to $(\beta, \beta p, \lambda)$, where $\beta \equiv 1/(k_B T)$ and $\lambda \equiv e^{\beta\mu}$. The equilibrium probability of finding the system in a microstate j with energy, volume, and number of particles (E_j, V_j, N_j) is

$$p_j = \frac{e^{-\beta(E_j + pV_j - \mu N_j)}}{\sum_j e^{-\beta(E_j + pV_j - \mu N_j)}} = \frac{1}{Y} e^{-\beta(E_j + pV_j - \mu N_j)}, \tag{22.21}$$

where $Y(\beta, \beta p, \lambda) = \sum_j e^{-\beta(E_j + pV_j - \mu N_j)}$ is the generalized partition sum. The bridge equation with thermodynamics is $\mathcal{E} = -k_B T \ln Y$. Thus, from Y and

$$d(\beta\mathcal{E}) = -d\ln Y = Ud\beta + \langle V\rangle\, d(\beta p) - \langle N\rangle\, d(\ln\lambda), \tag{22.22}$$

all equilibrium state functions can be obtained, such as

$$U = -\left(\frac{\partial \ln Y}{\partial \beta}\right)_{\beta p,\lambda}, \langle V\rangle = -\left(\frac{\partial \ln Y}{\partial(\beta p)}\right)_{\beta,\lambda},$$
$$\langle N\rangle = \lambda\left(\frac{\partial \ln Y}{\partial \lambda}\right)_{\beta,\beta p}. \tag{22.23}$$

Note that all extensive quantities, including $S/k_B = -\beta\mathcal{E} + \beta U + \beta p\langle V\rangle - \beta\mu\langle N\rangle$, $G = \mu\langle N\rangle + \mathcal{E}$, etc., are functions of the intensive variables (T, p, μ) or $(\beta, \beta p, \lambda)$ only. Intensive quantities are local fields whose gradients determine the fluxes of the extensive quantities. However, their size dependence is not the same as in classical thermodynamics. Thus, e.g., the expression $\langle N\rangle(T, p, \mu)$ can be solved for the chemical potential, which is then shown to depend on the system size, $\mu(T, p, \langle N\rangle)$.

The nanocanonical ensemble can only be used in nanosystems. Since Y does not depend on any extensive variable, the thermodynamic limit cannot be considered. This is logical, as (T, p, μ) are not independent variables and $\mathcal{E}$ is negligible in macroscopic systems.

22.3.2 Physical Interpretation of Nonlinear Corrections to the Boltzmann Factor

The Boltzmann distribution describes the occupation probability of different microstates of a system that only interacts thermally with an ideal reservoir that is able to fix the temperature by virtue of its practically infinite heat capacity and an instantaneous energy transfer between different parts of the system. However, deviations from this ideal situation may occur. For example, the "effective" number of degrees of freedom of the bath can be finite, as far as the thermal interaction with the system is concerned. Hence, corrections to the Boltzmann factor are necessary, as described in the next section.

22.3.3 Beck and Cohen's Superstatistics and Tsallis' Thermostatistics

Consider an ensemble collection of nanosystems in quasi-thermodynamic equilibrium with a thermal bath of temperature T_0. Because the temperature fluctuations of the nanosystems are important, two statistics must be superposed to describe the ensemble: the Boltzmann statistics $e^{-\beta E_j}$ and the probability distribution of $\beta = 1/(k_B T)$. The generalized probability distribution must be found by averaging over β. The effective Boltzmann factor is

$$B(E_j) = \int_0^\infty f(\beta) e^{-\beta E_j} d\beta, \tag{22.24}$$

where $f(\beta)$ is the probability distribution function of β, and the occupation probability of microstate j is

$$p(E_j) = \frac{B(E_j)}{\int_0^\infty B(E_j) dE_j} \equiv \frac{1}{Z_B} B(E_j). \tag{22.25}$$

This expression generalizes the Boltzmann canonical distribution, $p_j = e^{-\beta E_j}/Z$. The superstatistics approach [Beck and Cohen, 2003] is useful in many situations. For example, spatio-temporal fluctuations in temperature (or in other intensive magnitudes) may arise in driven nonequilibrium system under steady-state conditions. Spatial regions with different values of β would then play the role of different nanosystems.

The χ^2 or Γ (normalized) probability distribution

$$f(\beta) = \frac{1}{\Gamma(\gamma)} \frac{(\gamma\beta/\langle\beta\rangle)^\gamma e^{-\gamma\beta/\langle\beta\rangle}}{\beta} \propto \beta^{\gamma-1} e^{-\gamma\beta/\langle\beta\rangle}, \tag{22.26}$$

where $\Gamma(\gamma) = \int_0^\infty e^{-t} t^{\gamma-1} dt = (\gamma-1)!$ is the gamma function, is often observed in experiments. The two parameters of $f(\beta)$ are the average $\langle\beta\rangle = \int_0^\infty \beta f(\beta) d\beta$ and $\gamma \geq 0$. The latter is the reciprocal of the squared relative fluctuation of β. Thus, fluctuations increase with increasing $1/\gamma = \langle\beta^2\rangle / \langle\beta\rangle^2 - 1$.

The bath fixes the average temperature $\langle\beta\rangle = 1/(k_B T_0)$, but temperature fluctuations can occur, and the effective Boltzmann factor of the χ^2 distribution is then

$$B(E_j) = \int_0^\infty f(\beta) e^{-\beta E_j} d\beta = e_q^{-\langle\beta\rangle E_j}, \tag{22.27}$$

where $q \equiv 1 + 1/\gamma \geq 1$ is the entropic index and $e_q^x \equiv [1 + (1-q)x]^{1/(1-q)}$ is the Tsallis q-exponential [Tsallis, 2009,Naudts, 2011]. Although Tsallis distributions may originate from other reasons than temperature fluctuations, we have ended up with Tsallis statistics in a natural way, thus showing that the superstatistics approach contains Tsallis statistics as a particular case.

Phenomena characterized by probability distributions similar to Eq. (22.27) abound in nature. This type of statistics may arise from the convolution of the normal distribution with either a gamma or a power-law distribution, the latter being, for instance, a manifestation of the polydispersity of the system [Gheorghiu and Coppens, 2004].

The probability distribution $\{p_j\}$ can be transformed to $\{p_j^q\}$ by introducing an entropic index q as an exponent [Tsallis, 2009]. A microstate j with relatively small (large) probability p_j is a rare (frequent) event. The bias introduced by an index $q < 1$ is such that rare (frequent) events are promoted (restrained) because the probability $p_j^q / \sum_j p_j^q$ of microstate j in $\{p_j^q\}$ is larger than p_j if p_j is relatively small (smaller than p_j if p_j is relatively large). The opposite bias is introduced by an index $q > 1$. The simplest entropic form S_q that is a function of $\sum_j p_j^q$ and satisfies the conditions $\lim_{q\to 1} S_q = -k_B \sum_j p_j \ln p_j = S_{Gibbs}$ and $S_q = 0$, when all microstates but one has zero probability, is Tsallis entropy [Tsallis, 1988]

$$S_q = k \frac{\sum_j p_j^q - 1}{1 - q}. \tag{22.28}$$

The constant k is different from Boltzmann's constant but reduces to it when $q \to 1$. The entropic parameter q can be interpreted in terms of a fractal dimension for the attainable phase space [García-Morales and Pellicer, 2006]. With this interpretation, $0 \leq q \leq 1$. At the nanoscale, ions may have a reduced mobility close to highly charged interfaces (as a consequence of correlations), and a generalized Poisson–Boltzmann equation [García-Morales et al., 2004], obtained replacing the Boltzmann factor by an effective Tsallis factor with an entropic parameter $0 \leq q \leq 1$, has been shown to agree well with numerical simulations on highly charged planar interfaces.

Tsallis entropy includes the Boltzmann entropy and the Gibbs entropy equations as particular cases when $q \to 1$ as it can be transformed to

$$S_q = k \sum_j p_j \frac{(1/p_j)^{1-q} - 1}{1 - q} = k \sum_j p_j \ln_q \frac{1}{p_j}, \tag{22.29}$$

and the q-logarithm

$$\ln_q x \equiv \frac{x^{1-q}-1}{1-q} \tag{22.30}$$

becomes a natural logarithm when $q \to 1$, $\lim_{q\to 1} \ln_q x = \ln x$.

Tsallis entropy is claimed to be useful in cases where there are strong correlations between the microstates of different parts of a system [Cartwright, 2014]. Consider two systems A and B which are not independent, meaning that the probability of finding system B in microstate j_B depends on the microstate j_A in which system A is. This situation occurs, for instance, where there are interactions between the components of A and those of B. In this case, the probabilities of the microstates of $A+B$ do not factorize into those of A and B, $p_j \neq p^A_{j_A} p^B_{j_B}$, and the Gibbs entropy is not additive $S(A+B) \neq S(A)+S(B)$. According to Tsallis, the impossibility of keeping Gibbs entropy (additive and) extensive in cases like this is the crucial point of its theory [Cartwright, 2014]. In general, regardless of whether $p_j = p^A_{j_A} p^B_{j_B}$ or $p_j \neq p^A_{j_A} p^B_{j_B}$, Tsallis entropy is non-additive. However, there is one particular value q_{ent} that preserves the additivity

$$S_{q_{ent}}(A+B) = S_{q_{ent}}(A) + S_{q_{ent}}(B) \tag{22.31}$$

in the case of non-independent systems A and B [Tsallis, 2005, Tsallis, 2009].

22.3.4 Einstein's Theory of Fluctuations

Thermal fluctuations play a dominant role in nanothermodynamics. The equilibrium fluctuations of extensive quantities can be calculated, in statistical thermodynamics, from the partition sum. The occupation probability of a microstate (X_j, Y_j) when the environment fixes the intensive variables βx and βy is $p_j = e^{\beta x X_j} e^{\beta y Y_j}/Z$, where $Z = \sum_j e^{\beta x X_j} e^{\beta y Y_j}$ is the partition sum; typical examples of pairs of conjugate quantities in entropic representation are $\beta = 1/(k_B T)$ and $-E_j$, βp and $-V_j$, and $\beta\mu$ and N_j. The variance of, e.g., X around its average value $\langle X\rangle = (\partial \ln Z/\partial(\beta x))_{\beta y}$ is $\sigma^2_X = \langle X^2\rangle - \langle X\rangle^2 = (\partial \langle X\rangle/\partial(\beta x))_{\beta y}$. Typical examples of these fluctuation relations are $\sigma^2_E = k_B T^2 C_V$, $\sigma^2_H = k_B T^2 C_p$, $\sigma^2_V = k_B T \langle V\rangle \kappa_T$, etc. This approach cannot be used when the system is isolated, and Einstein's theory of fluctuations must then be used instead.

The second law states that, during its relaxation toward equilibrium, the entropy of an isolated system satisfies $(\partial S/\partial n)_{U,V,N} dn \geq 0$ where (U,V,N) remain fixed and the change in an internal variable n describes the advance of the process. The equilibrium condition $(\partial S/\partial n)_{U,V,N} = 0$ determines $n_{\rm eq}(U,V,N)$ and $S_{\rm eq}(U,V,N) = S(U,V,N,n_{\rm eq})$. However, fluctuations in n around $n_{\rm eq}$ also occur at equilibrium.

The probability of observing a macrostate (U,V,N,n) is proportional to its multiplicity, $p(n) \propto W(n)$. Boltzmann's equation $S(n) = k_B \ln W$ for isolated systems then implies

$$\frac{p(n)}{p(n_{\rm eq})} = \frac{W(n)}{W(n_{\rm eq})} = e^{(S-S_{\rm eq})/k_B}. \tag{22.32}$$

The expansion of $S(n)$ around $n_{\rm eq}$, truncated to second order, is

$$S = S_{\rm eq} + \frac{1}{2}\left(\frac{\partial^2 S}{\partial n^2}\right)_{\rm eq} (n-n_{\rm eq})^2 \tag{22.33}$$

because $(\partial S/\partial n)_{\rm eq} = 0$. The symmetry of $S - S_{\rm eq}$ around $n = n_{\rm eq}$ implies that $\langle n\rangle = n_{\rm eq}$. The probability distribution is Gaussian

$$p(n) = \frac{\exp\left[-\left(n-\langle n\rangle\right)^2/(2\sigma^2)\right]}{2\int_{\langle n\rangle}^{\infty} \exp\left[-\left(n-\langle n\rangle\right)^2/(2\sigma^2)\right] dn}, \tag{22.34}$$

and the variance of n is $\sigma^2 \equiv -k_B/(\partial^2 S/\partial n^2)_{\rm eq} = \langle n^2\rangle - \langle n\rangle^2$; note that $(\partial^2 S/\partial n^2)_{\rm eq} \leq 0$ because $S(n)$ is maximal at $n = n_{\rm eq}$. For example, for a closed system at constant volume, and with constant isochoric heat capacity, the variance of temperature is $\sigma^2_T = \langle T^2\rangle - \langle T\rangle^2 = -k_B/(\partial^2 S/\partial T^2)_{V,N} = k_B T^2/C_V$. Thus, temperature measurements with nanoscale resolution [Brites et al., 2012] are limited by the need to sample a minimum isochoric heat capacity. Similarly, when C_V becomes small due to quantum effects at low T, temperature fluctuations are dominant [Mafé et al., 2000]. Einstein's theory of fluctuations can also be applied to non-isolated systems, but corrections are necessary for very small systems [Falcioni et al., 2011]. Both in classical statistical thermodynamics and in Einstein's theory, the relative fluctuations scale with the reciprocal of the square root of the system size when the interaction with the environment fixes, at least, one extensive variable. On the contrary, systems with a completely open interaction with their surroundings exhibit relative fluctuations of the order of unity [Hill and Chamberlin, 2002].

22.4 Nonequilibrium Nanothermodynamics

22.4.1 Markov Processes: The Master Equation

Chemical reactions frequently take place on nanoscale physical systems and constitute fundamental examples of microscopic stochastic events [Gillespie, 1976, Gillespie, 1977]. In macroscopic systems, the chemical kinetics is completely determined by the concentrations of chemical species and by the reaction rate constants. Starting from a known initial condition, the chemical kinetics provides deterministic evolution laws for the concentrations, yielding a system trajectory on the phase space spanned by these dynamical variables. At the nanoscale, however, fluctuations of the numbers of particles on small volumes are large, and knowledge of the concentrations alone does not suffice to describe the evolution of the system. The macroscopic,

deterministic reaction kinetics breaks down in this case, and the stochastic character of chemical reactions produces significant deviations from the macroscopic average concentrations. Knowledge on the probability distribution of the number of particles and its evolution over time is, therefore, required in this case, to describe the system dynamics. The chemical master equation [Nicolis, 1972, Nicolis and Prigogine, 1977] constitutes the rigorous and general mathematical expression that allows one to address this problem. Since not all stochastic processes at the nanoscale are of chemical origin, we devote this chapter to derive and study an even more general expression, simply called the master equation from which the chemical master equation is a particular instance. Because of its major importance, the master equation is discussed in detail in now classical texts on stochastic processes [van Kampen, 2007,Gardiner, 2009], being also the subject of entire monographs [Oppenheim et al., 1977,Haag, 2017].

Let us consider a system described by a vector of stochastic variables $\mathbf{X}(t)$, and let $\mathbf{x}_0$ denote a random value of this vector measured at the 'present' time t_0. In chemical systems, these stochastic variables correspond to the numbers of particles of the chemical species, and thus they can take a discrete set of values, as we shall assume hereinafter. Let $\mathbf{x}_n$, $\mathbf{x}_{n-1}$, ..., $\mathbf{x}_1$ be random values of $\mathbf{X}(t)$ measured at future times $t_n > t_{n-1} > \ldots > t_1$ and let $\mathbf{x}_{-1}$, $\mathbf{x}_{-2}$, ... be those measured at past times $t_{-1} > t_{-2} > \ldots$. The stochastic evolution of the system is completely determined by the knowledge of the joint probability density

$$p\left(\mathbf{x}_n, t_n; \mathbf{x}_{n-1}, t_{n-1}; \ldots\right). \tag{22.35}$$

Summing over all mutually exclusive events that are possible for $\mathbf{x}_k$ at a certain time t_k in a joint probability distribution eliminates the dependence on $\mathbf{x}_k$ and t_k,

$$\begin{aligned}\sum_{\mathbf{x}_k} p\left(\ldots \mathbf{x}_{k+1}, t_{k+1}; \mathbf{x}_k, t_k; \mathbf{x}_{k-1}, t_{k-1}; \ldots\right) \\ = p\left(\ldots \mathbf{x}_{k+1}, t_{k+1}; \mathbf{x}_{k-1}, t_{k-1}; \ldots\right).\end{aligned} \tag{22.36}$$

The conditional probability density

$$p\left(\mathbf{x}_n, t_n; \ldots; \mathbf{x}_1, t_1 | \mathbf{x}_0, t_0; \mathbf{x}_{-1}, t_{-1}; \ldots\right) \tag{22.37}$$

is defined as the probability of measuring values $\mathbf{x}_n$, $\mathbf{x}_{n-1}$, ..., $\mathbf{x}_1$ for the stochastic vector at the corresponding future times, provided that the values of $\mathbf{x}_0$ and $\mathbf{x}_{-1}$, $\mathbf{x}_{-2}$, ... are known. The conditional probability density is given in terms of the joint probability density by

$$\begin{aligned}p\left(\mathbf{x}_n, t_n; \ldots; \mathbf{x}_1, t_1 | \mathbf{x}_0, t_0; \mathbf{x}_{-1}, t_{-1}; \ldots\right) \\ = \frac{p\left(\mathbf{x}_n, t_n; \mathbf{x}_{n-1}, t_{n-1}; \ldots\right)}{p\left(\mathbf{x}_0, t_0; \mathbf{x}_{-1}, t_{-1}; \ldots\right)}.\end{aligned} \tag{22.38}$$

These valid general expressions are of little practical value, and some assumptions are needed in order to come up with meaningful models of experimental systems. A simple assumption is *complete independence* of the stochastic processes, in which case the probability at time t does not depend on past values (nor on future ones). In this case, we have

$$p\left(\mathbf{x}_n, t_n; \mathbf{x}_{n-1}, t_{n-1}; \ldots\right) = \prod_{k=-\infty}^{n} p\left(\mathbf{x}_k, t_k\right). \tag{22.39}$$

If the independent probabilities $p\left(\mathbf{x}_k, t_k\right)$ do not depend on t_k, one has the even more simple special case of *Bernoulli trials*. A less simple stochastic process is the *Markov process* for which the joint probability density is given by

$$p\left(\mathbf{x}_n, t_n; \mathbf{x}_{n-1}, t_{n-1}; \ldots\right) = \prod_{k=-\infty}^{n} p\left(\mathbf{x}_k, t_k | \mathbf{x}_{k-1}, t_{k-1}\right). \tag{22.40}$$

From Eq. (22.40) we have, by using Eq. (22.38),

$$\begin{aligned}p\left(\mathbf{x}_n, t_n; \mathbf{x}_{n-1}, t_{n-1}; \ldots | \mathbf{x}_0, t_0; \mathbf{x}_{-1}, t_{-1}; \ldots\right) \\ = p\left(\mathbf{x}_n, t_n; \mathbf{x}_{n-1}, t_{n-1}; \ldots | \mathbf{x}_0, t_0\right).\end{aligned} \tag{22.41}$$

This is called the *Markov assumption*: knowledge of the future depends on knowledge of the present only. This is, of course, an idealization, but there may be systems whose memory time is small enough so that, if we carry out our observations on a longer time scale, it is fair to approximate them by a Markov process.

The Markov assumption allows one to reduce all considerations of the stochastic evolution to the knowledge of the initial probability density and the conditional probability density. Indeed, if one knows the initial probability distribution $p(\mathbf{x}_0, t_0)$, one has that, at a later time t_1, the following relationship holds

$$p(\mathbf{x}_1, t_1) = \sum_{\mathbf{x}_0} p(\mathbf{x}_1, t_1 | \mathbf{x}_0, t_0) p(\mathbf{x}_0, t_0), \tag{22.42}$$

i.e., the initial probability distribution at time t_0 is 'propagated' to time t_1 through the conditional probability density. Let us write $\mathbf{x} \equiv \mathbf{x}_0$ and $\mathbf{y} \equiv \mathbf{x}_1$. If we also put $t_0 \equiv t$ and $t_1 \equiv t' = t + dt$, where dt is an infinitesimally small time increment, we have

$$\begin{aligned}p(\mathbf{y}, t + dt) &= \sum_{\mathbf{x}} p(\mathbf{y}, t + dt | \mathbf{x}, t) p(\mathbf{x}, t) \\ &= \sum_{\mathbf{x}} \left(p(\mathbf{y}, t | \mathbf{x}, t) + dt \left. \frac{\partial p(\mathbf{y}, t' | \mathbf{x}, t)}{\partial t'} \right|_{t'=t} \right) p(\mathbf{x}, t) \\ &= \sum_{\mathbf{x}} \left(\delta_{\mathbf{yx}} + dt \left. \frac{\partial p(\mathbf{y}, t' | \mathbf{x}, t)}{\partial t'} \right|_{t'=t} \right) p(\mathbf{x}, t) \\ &= p(\mathbf{y}, t) + dt \sum_{\mathbf{x}} \left. \frac{\partial p(\mathbf{y}, t' | \mathbf{x}, t)}{\partial t'} \right|_{t'=t} p(\mathbf{x}, t),\end{aligned} \tag{22.43}$$

where we have used that

$$p(\mathbf{y}, t | \mathbf{x}, t) = \delta_{\mathbf{yx}} \tag{22.44}$$

(with $\delta_{\mathbf{yx}} = 1$ if $\mathbf{y} = \mathbf{x}$ and $\delta_{\mathbf{yx}} = 0$ otherwise) because at time t_0, we specify that $\mathbf{X}(t_0) = \mathbf{x}$ in the conditional

probability density. From Eq. (22.43), we thus obtain

$$\frac{\partial p(\mathbf{y},t)}{\partial t} = \sum_{\mathbf{x}} \left.\frac{\partial p(\mathbf{y},t'|\mathbf{x},t)}{\partial t'}\right|_{t'=t} p(\mathbf{x},t). \tag{22.45}$$

Since we also have

$$\sum_{\mathbf{y}} p(\mathbf{y},t+dt|\mathbf{x},t) = \sum_{\mathbf{y}} \frac{p(\mathbf{y},t+dt;\mathbf{x},t)}{p(\mathbf{x},t)} = 1 \tag{22.46}$$

and, from Eq. (22.43),

$$\begin{aligned}\sum_{\mathbf{y}} p(\mathbf{y},t+dt|\mathbf{x},t) &= \sum_{\mathbf{y}} \left(\delta_{\mathbf{yx}} + dt \left.\frac{\partial p(\mathbf{y},t'|\mathbf{x},t)}{\partial t'}\right|_{t'=t}\right) \\ &= 1 + dt \sum_{\mathbf{y}} \left.\frac{\partial p(\mathbf{y},t'|\mathbf{x},t)}{\partial t'}\right|_{t'=t},\end{aligned} \tag{22.47}$$

necessarily

$$\sum_{\mathbf{y}} \left.\frac{\partial p(\mathbf{y},t'|\mathbf{x},t)}{\partial t'}\right|_{t'=t} = 0. \tag{22.48}$$

This latter equation is equivalent to

$$\left.\frac{\partial p(\mathbf{x},t'|\mathbf{x},t)}{\partial t'}\right|_{t'=t} = -\sum_{\mathbf{y}(\mathbf{y}\neq\mathbf{x})} \left.\frac{\partial p(\mathbf{y},t'|\mathbf{x},t)}{\partial t'}\right|_{t'=t}, \tag{22.49}$$

and, therefore, we can generally write

$$\begin{aligned}\left.\frac{\partial p(\mathbf{y},t'|\mathbf{x},t)}{\partial t'}\right|_{t'=t} &\equiv \mathbb{W}_{\mathbf{yx}} \\ &\equiv \begin{cases} W(\mathbf{y}|\mathbf{x},t) & \text{if } \mathbf{y}\neq\mathbf{x}, \\ W(\mathbf{y}|\mathbf{x},t) - \sum_{\mathbf{x}'} W(\mathbf{x}'|\mathbf{x},t) & \text{if } \mathbf{y}=\mathbf{x}, \end{cases}\end{aligned} \tag{22.50}$$

where we have introduced the transition (or jump) probability per unit time $W(\mathbf{y}|\mathbf{x},t)$. We can bring the two parts of Eq. (22.50) together in a single equation as

$$\left.\frac{\partial p(\mathbf{y},t'|\mathbf{x},t)}{\partial t'}\right|_{t'=t} = W(\mathbf{y}|\mathbf{x},t) - \delta_{\mathbf{yx}} \sum_{\mathbf{x}'} W(\mathbf{x}'|\mathbf{x},t). \tag{22.51}$$

By replacing Eq. (22.51) in (22.45), we finally obtain the celebrated master equation

$$\begin{aligned}\frac{\partial p(\mathbf{y},t)}{\partial t} &= \sum_{\mathbf{x}} W(\mathbf{y}|\mathbf{x},t)p(\mathbf{x},t) - \sum_{\mathbf{x}'} W(\mathbf{x}'|\mathbf{y},t)p(\mathbf{y},t) \\ &= \sum_{\mathbf{x}} \mathbb{W}_{\mathbf{yx}} p(\mathbf{x},t).\end{aligned} \tag{22.52}$$

This equation admits a straightforward interpretation. The change in time of the probability of observing a state $\mathbf{y}$ is composed of two contributions: a positive term that accounts for the incoming probability flow in which state $\mathbf{y}$ is reached from any other state $\mathbf{x}$ and a negative contribution that describes the outgoing probability flow in which state $\mathbf{y}$ is left for any other state $\mathbf{x}'$. The transition rates $W(\mathbf{y}|\mathbf{x},t)$ contain all known information about the stochastic system and can be often inferred from phenomenological considerations. Thanks to the master equation we can know the time evolution of the average $\langle f(\mathbf{y})\rangle \equiv \sum_{\mathbf{y}} f(\mathbf{y})p(\mathbf{y},t)$ of any function f of the stochastic variable $\mathbf{y}$, since

$$\frac{d\langle f(\mathbf{y})\rangle}{dt} = \sum_{\mathbf{y}} f(\mathbf{y}) \frac{\partial p(\mathbf{y},t)}{\partial t} = \sum_{\mathbf{y}} \sum_{\mathbf{x}} f(\mathbf{y}) \mathbb{W}_{\mathbf{yx}} p(\mathbf{x},t). \tag{22.53}$$

In nanoscale systems, chemical reactions make the number N_i of reacting species i fluctuate as it is produced/consumed at random, each time a specific reaction takes place. Suppose that there are s reacting species. The state of a chemical system at a time t is, thus, specified by a value of the stochastic vector $\mathbf{N} = (N_1,\ldots,N_i,\ldots,N_s)$ containing the numbers of particles present in the reaction tank at that time. Since several chemical reactions may occur, let an index ρ be used to label them. Any such reaction has the general form

$$\sum_{i=1}^{s} \nu^i_{<\rho} N_i \xrightarrow{k_\rho} \sum_{i=1}^{s} \nu^i_{>\rho} N_i. \tag{22.54}$$

Here we have introduced the numbers for each chemical species i entering in a reaction ρ as a reactant $\nu^i_{<\rho}$ or as a product $\nu^i_{>\rho}$ of that reaction. Thus, the number of particles of species i being produced through reaction ρ is given by the stoichiometric coefficients ν^i_ρ which correspond to the difference of these numbers, i.e., $\nu^i_\rho \equiv \nu^i_{>\rho} - \nu^i_{<\rho}$. As it is the case with the number of particles, for each reaction ρ, we can put all s stoichiometric coefficients in a vector $\nu_\rho = (\nu^1_\rho,\ldots,\nu^i_\rho,\ldots,\nu^s_\rho)$. The rate at which the particles are created or annihilated is given by the reaction rate constant k_ρ. We can now ask what the probability $P(\mathbf{N},t)$ at time t of observing a value $\mathbf{N}$ for the numbers of particles in the system is. We note that the state $\mathbf{N}$ can be reached from a state $\mathbf{N}-\nu_\rho$ and can be left to a state $\mathbf{N}+\nu_\rho$. Thus, by taking $\mathbf{y}=\mathbf{N}$ in the master equation, Eq. (22.52), and $\mathbf{x}=\mathbf{N}-\nu_\rho$, we obtain the chemical master equation

$$\begin{aligned}\frac{\partial p(\mathbf{N},t)}{\partial t} = \sum_{\rho} \big[&W_\rho(\mathbf{N}|\mathbf{N}-\nu_\rho)\; p(\mathbf{N}-\nu_\rho,t) \\ &- W_\rho\;(\mathbf{N}+\nu_\rho|\mathbf{N})p(\mathbf{N},t)\big].\end{aligned} \tag{22.55}$$

The jump probabilities $W_\rho(\mathbf{N}-\nu_\rho|\mathbf{N})$ per unit time of a chemical system are called propensities [Gillespie, 1977] and are specific for the reaction ρ. They are proportional to the reaction rate constant k_ρ and to the numbers of particles involved in the relevant reaction event. If we assume Ω to be the volume of the reaction tank, the probability of finding a molecule of species i is thus proportional to N_i/Ω. The probability of finding a different second molecule of the same species is then proportional to $(N_i-1)/\Omega$. Since in reaction ρ there are $\nu^i_{<\rho}$ reactant molecules involved, the probability of finding all of them in a reaction event is, therefore, proportional to the product of all these probabilities, i.e., $N_i(N_i-1)\ldots(N_i-\nu^i_{<\rho}+1)/\Omega^{\nu^i_{<\rho}}$. Therefore, the propensities are given by the following expression

$$W_\rho(\mathbf{N}+\nu_\rho|\mathbf{N}) = \Omega k_\rho \prod_{i=1}^{s} \prod_{m=1}^{\nu^i_{<\rho}} \frac{N_i - m + 1}{\Omega}. \tag{22.56}$$

Let us take the Brusselator as an example. The chemical reactions involving two chemical species X and Y are [Gaspard, 2002]

$$\xrightarrow{k_1} \quad X, \tag{22.57}$$

$$X \xrightarrow{k_2} Y, \tag{22.58}$$

$$2X + Y \xrightarrow{k_3} 3X, \tag{22.59}$$

$$X \xrightarrow{k_4} \quad . \tag{22.60}$$

If we denote by X and Y the number of particles of the corresponding chemical species, the state of the system is given by the vector $\mathbf{N} = (X, Y)$, and we find that, for this system, the vectors containing the number of reactant particles $\nu_{<\rho} = (\nu^1_{<\rho}, \nu^2_{<\rho})$ and stoichiometric coefficients $\nu_\rho = (\nu^1_\rho, \nu^2_\rho)$ are

$$\nu_{<1} = (0,0) \quad \nu_{<2} = (1,0) \quad \nu_{<3} = (2,1) \quad \nu_{<4} = (1,0)\,, \tag{22.61}$$

$$\nu_1 = (1,0) \quad \nu_2 = (-1,1) \quad \nu_3 = (1,-1) \quad \nu_4 = (-1,0)\,. \tag{22.62}$$

Therefore, for this system, the propensities are readily calculated from Eq. (22.56) as

$$W_1(\mathbf{N}+\nu_1|\mathbf{N}) = \Omega k_1 \;\; W_2(\mathbf{N}+\nu_2|\mathbf{N}) = k_2 X,$$
$$W_3(\mathbf{N}+\nu_3|\mathbf{N}) = k_3 X(X-1)Y/\Omega^2 \;\; W_4(\mathbf{N}+\nu_4|\mathbf{N}) = k_4 X. \tag{22.63}$$

And, thus, by replacing Eq. (22.63) in the chemical master equation Eq. (22.55), the time evolution of the probability distribution $p(\mathbf{N}, t)$ can be numerically obtained. We shall come back to this problem in Section 22.4.4 providing explicit simulation results for the Brusselator. In the next section, we exploit the master equation to derive some further important results of interest in the statistical modeling of nanoscale systems.

22.4.2 Fluctuation Theorems and Irreversibility

The master equation has always, at least, one nontrivial stationary state for the probability distribution $p_{\rm st}(\mathbf{y})$. This can be proved by observing that at the stationary state, one has, from Eq. (22.52),

$$\begin{aligned} 0 &= \sum_{\mathbf{x}} W(\mathbf{y}|\mathbf{x},t) p_{\rm st}(\mathbf{x}) - \sum_{\mathbf{x}'} W(\mathbf{x}'|\mathbf{y},t) p_{\rm st}(\mathbf{y}) \\ &= \sum_{\mathbf{x}} \mathbb{W}_{\mathbf{yx}} p_{\rm st}(\mathbf{x}), \end{aligned} \tag{22.64}$$

which is a linear algebraic equation that has a nontrivial solution $p_{\rm st}(\mathbf{x}) \neq 0$ if the determinant of the matrix $\mathbb{W}_{\mathbf{yx}}$ vanishes. But this is always the case because, from Eq. (22.48), not all row vectors of the matrix $\mathbb{W}_{\mathbf{yx}}$ are independent.

If there is a finite number of discrete states, a probability distribution governed by the master equation will always tend to one of its stationary states in the infinite time limit [van Kampen, 2007]. Let us study in more detail some fundamental thermodynamic implications of the evolution in phase space of any system governed by a master equation. Let $P(\mathbf{y}, t)$ denote the probability that after a time interval t, such a system has undergone no transition from its original state $\mathbf{y}$. Then, after a further infinitesimal time increment τ, the probability $P(t+\tau)$ that the system still remains in the same state is

$$\begin{aligned} P(\mathbf{y}, t+\tau) &= p(\mathbf{y}, t+\tau|\mathbf{y}, t) P(\mathbf{y}, t) \\ &= P(\mathbf{y}, t) \left(p(\mathbf{y}, t|\mathbf{y}, t) + \tau \left. \frac{\partial p(\mathbf{y}, t'|\mathbf{y}, t)}{\partial t'} \right|_{t'=t} \right) \\ &= P(\mathbf{y}, t) \left(1 - \tau \sum_{\mathbf{x}' \neq \mathbf{y}} W(\mathbf{x}'|\mathbf{y}, t) \right), \end{aligned} \tag{22.65}$$

where Eq. (22.49) with $\mathbf{x} = \mathbf{y}$ has been used. Note that the quantity within parentheses corresponds to the probability that no transition has occurred provided that we know with certainty that, at time t, the state is $\mathbf{y}$. Therefore, in the limit $\tau \to 0$, we obtain

$$\frac{\partial P(\mathbf{y}, t)}{\partial t} = -P(\mathbf{y}, t) \sum_{\mathbf{x}' \neq \mathbf{y}} W(\mathbf{x}'|\mathbf{y}, t), \tag{22.66}$$

which can be integrated to give

$$P(\mathbf{y}, t) = \exp\left(- \sum_{\mathbf{x}' \neq \mathbf{y}} \int_{t_0}^{t_0+t} W(\mathbf{x}'|\mathbf{y}, t') dt' \right) \tag{22.67}$$

because $P(\mathbf{y}, 0) = 1$.

The master equation allows us to know the probability distribution at every time, and hence, we can define the probability $p(\mathbf{y}_0 \to \mathbf{y}_n)$ that a given stochastic trajectory of duration $t = t_n - t_0$ joining the events $(\mathbf{y}_0, t_0)$, $(\mathbf{y}_1, t_1)$, …, $(\mathbf{y}_n, t_n)$ takes place. This is given the product of the joint probability distribution that, at every discrete time t_k, an event has happened (so that the state has made a transition from $\mathbf{y}_{k-1}$ to $\mathbf{y}_k$), multiplied by all probabilities that between two consecutive discrete events no other event has taken place:

$$\begin{aligned} p(\mathbf{y}_0 \to \mathbf{y}_n) &\equiv p\left(\mathbf{y}_n, t_n; \mathbf{y}_{n-1}, t_{n-1}; \ldots; \mathbf{y}_1, t_1\right) \\ &\quad \times \prod_{k=0}^{n-1} P(\mathbf{y}_k, t_{k+1} - t_k) \\ &= \prod_{k=1}^{n} p\left(\mathbf{y}_{k+1}, t_{k+1} | \mathbf{y}_k, t_k\right) P(\mathbf{y}_{k-1}, t_k - t_{k-1}). \end{aligned} \tag{22.68}$$

Here, Eq. (22.40) has been used. Since, obviously, $\mathbf{y}_{k+1} \neq \mathbf{y}_k$, for each $k = 0, \ldots, n-1$ (each single transition always

proceeds from a state to a different one), we have that $p\left(\mathbf{y}_{k+1}, t_{k+1}|\mathbf{y}_k, t_k\right) = (t_{k+1}-t_k)W(\mathbf{y}_{k+1}|\mathbf{y}_k, t_k)$. Therefore, by using Eq. (22.67), we obtain

$$p(\mathbf{y}_0 \to \mathbf{y}_n) = \prod_{k=1}^{n}(t_{k+1}-t_k)W(\mathbf{y}_{k+1}|\mathbf{y}_k, t_k) \exp\left(-\sum_{\mathbf{x}'\neq\mathbf{y}_k}\int_{t_{k-1}}^{t_k} W(\mathbf{x}'|\mathbf{y}_{k-1}, t')dt'\right). \tag{22.69}$$

The probability of observing the time-reversed trajectory, provided that we know that we start from $\mathbf{y}_n$, is given by

$$p(\mathbf{y}_n \to \mathbf{y}_0) = \prod_{k=1}^{n}(t_{k+1}-t_k)W(\mathbf{y}_k|\mathbf{y}_{k+1}, t-t_{k+1}) \exp\left(-\sum_{\mathbf{x}'\neq\mathbf{y}_k}\int_{t-t_k}^{t-t_{k-1}} W(\mathbf{x}'|\mathbf{y}_k, t')dt'\right). \tag{22.70}$$

Following [Seifert, 2005], we can now define the trajectory-dependent entropy of a path $\eta : \mathbf{y}_0 \to \mathbf{y}_1 \to \ldots \to \mathbf{y}_n$ connecting any initial condition $(\mathbf{x}_0, t_0)$ to a state $(\mathbf{x}_n, t_n)$ as

$$s(\eta) \equiv -\ln\left[p(\mathbf{y}_0, t_0)p(\mathbf{y}_0 \to \mathbf{y}_n)\right]. \tag{22.71}$$

By noting that

$$\sum_{\eta} p(\mathbf{y}_0, t_0)p(\mathbf{y}_0 \to \mathbf{y}_n) = 1, \tag{22.72}$$

the Gibbs–Shannon entropy is obtained by averaging $s(\eta)$ over all possible paths

$$\begin{aligned}\langle s(\eta)\rangle_\eta &\equiv -\sum_{\eta} p(\mathbf{y}_0, t_0)p(\mathbf{y}_0 \to \mathbf{y}_n)\ln\left[p(\mathbf{y}_0, t_0)p(\mathbf{y}_0 \to \mathbf{y}_n)\right] \\ &= S_{GS}.\end{aligned} \tag{22.73}$$

From here, we now note that the functional

$$R\left(\mathbf{y}_0 \to \mathbf{y}_n\right) = \ln\frac{p(\mathbf{y}_0, t_0)p(\mathbf{y}_0 \to \mathbf{y}_n)}{p(\mathbf{y}_n, t_n)p(\mathbf{y}_n \to \mathbf{y}_0)} = s(\eta')-s(\eta) = \Delta s_{\text{tot}} \tag{22.74}$$

denotes the total entropy difference between a trajectory η and its reverse counterpart η'. Therefore, by summing over all possible reverse trajectories η', we have

$$\begin{aligned}1 &= \sum_{\eta'} p(\mathbf{y}_n, t_n)p(\mathbf{y}_n \to \mathbf{y}_0) \\ &= \sum_{\eta'} p(\mathbf{y}_0, t_0)p(\mathbf{y}_0 \to \mathbf{y}_n)e^{-R(\mathbf{y}_0 \to \mathbf{y}_n)} \\ &= \sum_{\eta} p(\mathbf{y}_0, t_0)p(\mathbf{y}_0 \to \mathbf{y}_n)e^{-R(\mathbf{y}_0 \to \mathbf{y}_n)} \\ &= \left\langle e^{-R(\mathbf{y}_0 \to \mathbf{y}_n)}\right\rangle_\eta.\end{aligned} \tag{22.75}$$

Since, by Jensen's inequality [Chandler, 1987], $\langle e^{-x}\rangle \geq e^{-\langle x\rangle}$, this latter expression necessarily implies

$$\langle R\left(\mathbf{y}_0 \to \mathbf{y}_n\right)\rangle_\eta \geq 0, \tag{22.76}$$

and, therefore,

$$\langle \Delta s_{\text{tot}}\rangle_\eta \geq 0. \tag{22.77}$$

This expression constitutes the integral FT [Seifert, 2005], and it establishes that the average over all possible nonequilibrium paths for the total entropy change is non-negative. In the thermodynamic limit, and/or trajectories spanning over a long time, this theorem implies the Second Law of Thermodynamics. Out of the thermodynamic limit, the nanoscale being a paradigmatic domain, there is a significant non-zero probability of finding paths that make a negative contribution to the total entropy, although their total average contribution will still be positive. The integral FT provides an elegant explanation of the Loschmidt paradox, showing that the Second Law is a consequence of causality [Evans and Searles, 2002] and thus elucidating how macroscopic irreversible dynamics can arise out of microscopic reversible laws.

There has arisen a plethora of FTs since their discovery [Evans et al.; 1993], and there exists a vast literature on the subject. Any convex function defined over a trajectory will lead to functionals that satisfy an integral FT, analogous to the one sketched above for the trajectory entropy. This mathematical fact allows one to better understand how macroscopic thermodynamics can emerge out of statistical non-equilibrium laws and how macroscopic nonequilibrium thermodynamics can be transposed down to the nanoscale. An excellent recent review [Seifert, 2012] is strongly recommended for the interested reader.

22.4.3 Van Kampen's Volume Expansion and the Fokker–Planck Equation

The master equation can be systematically expanded in the low noise (large system size, $\Omega \to \infty$) approximation. Such expansion allows one to handle relevant, statistical corrections to macroscopic deterministic laws. In this way, the master equation provides a unified nonequilibrium picture ranging from systems consisting of a few molecules to macroscopic systems composed by an Avogadro's number of them.

Because of its great general interest for nanoscale systems, and because of the wide scope of its implications, we offer in detail the rigorous expansion of the master equation. Although we strictly adhere to van Kampen's approach [van Kampen, 2007], the full details of the expansion in [van Kampen, 2007] are there only explicitly given for an univariate chemical master equation, and only a specific example of multivariate expansion is worked out in detail. Here, we offer in full detail and generality van Kampen's expansion for the multivariate master equation. We do so in view of the interest of this approach for applications to chemical systems: the latter are usually composed of many different species and lead naturally to multivariate expressions. As magnificently elucidated by van Kampen, naive use of the popular Langevin approach or careless truncations of the Kramers–Moyal expansion, as found in an enormous number of references in the literature, leads easily to

paradoxes and unphysical results, and such paths should probably better be avoided.

The relative impact of fluctuations on macroscopic equilibrium thermodynamic quantities is proportional to the reciprocal of the square root of the system size Ω. This rigorous expansion consistently yields corrections proportional to powers of $\Omega^{-1/2}$. The expansion is valid for all systems in which transition probabilities per unit time have the following canonical form:

$$W(\mathbf{y}|\mathbf{x},t) = f(\Omega)\left[\phi_0\left(\frac{\mathbf{x}}{\Omega};\mathbf{r},t\right)+\frac{1}{\Omega}\phi_1\left(\frac{\mathbf{x}}{\Omega};\mathbf{r},t\right)+\frac{1}{\Omega^2}\phi_2+\ldots\right], \tag{22.78}$$

where $f(\Omega)$ is just an arbitrary function of Ω alone and the functions ϕ_j, $j=0,1,\ldots$ depend only on the 'intensive variables' $\mathbf{x}/\Omega$ and the jumps between states $\mathbf{r}\equiv\mathbf{y}-\mathbf{x}$. Most systems of physical interest have transition probabilities per unit time with the above canonical form. This is clearly the case of chemical systems, since the propensities in Eq. (22.56) are particular instances of Eq. (22.78) where we have $\mathbf{x}=\mathbf{N}$, $\mathbf{r}=\nu_\rho$, $f(\Omega)=\Omega$,

$$\phi_0 = k_\rho \prod_{i=1}^{s}\prod_{m=1}^{\nu^i_{\ell\rho}}\frac{N_i-m+1}{\Omega},$$
$$\phi_j = 0 \qquad (j>0). \tag{22.79}$$

We shall assume in the following expansion that any vector quantity under discussion (let us generically denote it by $\mathbf{v}$) has a number s of components, and we shall write v_j for the jth coordinate of the vector $\mathbf{v}$, so that we have $\mathbf{v}=(v_1,\ldots,v_{j-1},v_j,v_{j+1},\ldots,v_s)$.

By replacing Eq. (22.78) in (22.52), we have

$$\frac{\partial p(\mathbf{y},t)}{\partial t} = f(\Omega)\sum_{\mathbf{r}}\left[\phi_0\left(\frac{\mathbf{y}-\mathbf{r}}{\Omega};\mathbf{r},t\right)+\frac{1}{\Omega}\phi_1\left(\frac{\mathbf{y}-\mathbf{r}}{\Omega};\mathbf{r},t\right)+\ldots\right]\times p(\mathbf{y}-\mathbf{r},t) - f(\Omega)\sum_{\mathbf{r}}\left[\phi_0\left(\frac{\mathbf{y}}{\Omega};-\mathbf{r},t\right)+\frac{1}{\Omega}\phi_1\left(\frac{\mathbf{y}}{\Omega};-\mathbf{r},t\right)+\ldots\right]\times p(\mathbf{y},t). \tag{22.80}$$

The essential step in the expansion of the master equation comes from introducing an appropriate change of variables that anticipates some of the main broad features of the expected solution. This consists on splitting $\mathbf{y}$ into two contributions: one deterministic (that we shall fix through the macroscopic limit), which describes the average of the probability distribution, and the other stochastic (carrying all higher moments of the probability distribution). Therefore, the state $\mathbf{y}/\Omega=(y_1/\Omega,\ldots,y_s/\Omega)$ of the system is made dependent on time through a function $\mathbf{g}(t)=(g_1(t),\ldots,g_s(t))$ that is to be specified in the macroscopic limit $\Omega\to\infty$ and which describes the motion of the peak of the probability distribution $p(\mathbf{y},t)$ in that limit. The state also depends on the stochastic variable $\mathbf{w}=(w_1,\ldots,w_s)$ which evolves on the scale of the fluctuations of $\mathbf{y}/\Omega$ leading to deviations from the macroscopic average. In the thermodynamic limit, these fluctuations have a relative impact which is proportional to $\Omega^{-1/2}$:

$$\frac{\mathbf{y}}{\Omega} = \mathbf{g}(t)+\Omega^{-1/2}\mathbf{w}. \tag{22.81}$$

In this way, the probability distribution is described in terms of these new variables. We, therefore, write

$$\mathcal{P}(\mathbf{w},t)\equiv p(\mathbf{y},t)=p(\Omega\mathbf{g}(t)+\Omega^{1/2}\mathbf{w},t). \tag{22.82}$$

We note the following relationships involving the new and the old variables

$$\frac{\partial^k\mathcal{P}}{\partial w_{j_1}\partial w_{j_2}\ldots\partial w_{j_k}} = \Omega^{k/2}\frac{\partial^k p}{\partial y_{j_1}\partial y_{j_2}\ldots\partial y_{j_k}}, \tag{22.83}$$

$$\frac{\partial\mathcal{P}}{\partial t} = \frac{\partial p}{\partial t}+\Omega\sum_{j=1}^{s}\frac{dg_j}{dt}\frac{\partial p}{\partial y_j} = \frac{\partial p}{\partial t}+\Omega^{1/2}\sum_{j=1}^{s}\frac{dg_j}{dt}\frac{\partial\mathcal{P}}{\partial w_j}. \tag{22.84}$$

We have now all necessary ingredients to perform the expansion. By replacing Eqs. (22.81) and (22.82) in Eq. (22.52) and using Eq. (22.84), we obtain

$$\begin{aligned}\frac{\partial\mathcal{P}}{\partial t}-\Omega^{1/2}\sum_{j=1}^{s}\frac{dg_j}{dt}\frac{\partial\mathcal{P}}{\partial w_j} &= f(\Omega)\sum_{\mathbf{r}}\Big[\phi_0\left(\mathbf{g}(t)\right.\\ &+\Omega^{-1/2}(\mathbf{w}-\Omega^{-1/2}\mathbf{r});\mathbf{r},t\big)+\frac{1}{\Omega}\phi_1\left(\mathbf{g}(t)\right.\\ &+\Omega^{-1/2}(\mathbf{w}-\Omega^{-1/2}\mathbf{r});\mathbf{r},t\big)+\ldots\Big]\mathcal{P}(\mathbf{w}-\Omega^{-1/2}\mathbf{r},t)\\ &-f(\Omega)\sum_{\mathbf{r}}\Big[\phi_0\left(\mathbf{g}(t)+\Omega^{-1/2}\mathbf{w};-\mathbf{r},t\right)+\frac{1}{\Omega}\phi_1\left(\mathbf{g}(t)\right.\\ &+\Omega^{-1/2}\mathbf{w};-\mathbf{r},t\big)+\ldots\Big]\mathcal{P}(\mathbf{w},t).\end{aligned} \tag{22.85}$$

We now note that the second and third lines of Eq. (22.85) contain terms in which $\mathbf{w}$ is shifted by $-\Omega^{-1/2}\mathbf{r}$. By making a Taylor expansion of those terms around $\mathbf{w}$ in powers of $-\Omega^{-1/2}\mathbf{r}$, we find that terms of order zero are canceled by those in line 4 of Eq. (22.85). Therefore, we obtain

$$\begin{aligned}\frac{\partial\mathcal{P}}{\partial t}-\Omega^{1/2}\sum_{j=1}^{s}\frac{dg_j}{dt}\frac{\partial\mathcal{P}}{\partial w_j} &= -\Omega^{-1/2}f(\Omega)\sum_{\mathbf{r}}\sum_{j=1}^{s}\frac{\partial}{\partial w_j}r_j\phi_0\\ &\times\left(\mathbf{g}(t)+\Omega^{-1/2}\mathbf{w};\mathbf{r},t\right)\mathcal{P}(\mathbf{w},t)\\ &+\frac{1}{2}\Omega^{-1}f(\Omega)\sum_{\mathbf{r}}\sum_{j_1=1}^{s}\sum_{j_2=1}^{s}\frac{\partial^2}{\partial w_{j_1}\partial w_{j_2}}r_{j_1}r_{j_2}\phi_0\\ &\times\left(\mathbf{g}(t)+\Omega^{-1/2}\mathbf{w};\mathbf{r},t\right)\mathcal{P}(\mathbf{w},t)\\ &-\frac{1}{3!}\Omega^{-3/2}f(\Omega)\sum_{\mathbf{r}}\sum_{j_1=1}^{s}\sum_{j_2=1}^{s}\sum_{j_3=1}^{s}\frac{\partial^3}{\partial w_{j_1}\partial w_{j_2}\partial w_{j_3}}r_{j_1}r_{j_2}r_{j_3}\phi_0\end{aligned}$$

$$\times \left(\mathbf{g}(t) + \Omega^{-1/2}\mathbf{w}; \mathbf{r}, t\right) \mathcal{P}(\mathbf{w}, t)$$
$$- \Omega^{-3/2} f(\Omega) \sum_{\mathbf{r}} \sum_{j=1}^{s} \frac{\partial}{\partial w_j} r_j \phi_1$$
$$\times \left(\mathbf{g}(t) + \Omega^{-1/2}\mathbf{w}; \mathbf{r}, t\right) \mathcal{P}(\mathbf{w}, t) + \mathcal{O}(\Omega^{-2}). \quad (22.86)$$

We define the rescaled jump moments

$$\alpha_{km}^{(j_1 \cdots j_k)}(\mathbf{x}) \equiv \sum_{\mathbf{r}} r_{j_1} r_{j_2} \ldots r_{j_k} \phi_m(\mathbf{x}; \mathbf{r}, \tau). \quad (22.87)$$

In these expressions, the indices $j_1, \ldots, j_k$ are all free. Therefore, $\alpha_{1,0}^{(j)}$ corresponds to a vector, $\alpha_{2,0}^{(j_1 j_2)}$ to a matrix, etc. In terms of a rescaled time

$$\Omega^{-1} f(\Omega) t = \tau, \quad (22.88)$$

we find

$$\frac{\partial \mathcal{P}}{\partial \tau} - \Omega^{1/2} \sum_{j=1}^{s} \frac{dg_j}{d\tau} \frac{\partial \mathcal{P}}{\partial w_j} = -\Omega^{1/2} \sum_{j=1}^{s} \frac{\partial}{\partial w_j} \alpha_{1,0}^{(j)}$$
$$\times \left(\mathbf{g} + \Omega^{-1/2}\mathbf{w}\right) \mathcal{P}$$
$$+ \frac{1}{2} \sum_{j_1=1}^{s} \sum_{j_2=1}^{s} \frac{\partial^2}{\partial w_{j_1} \partial w_{j_2}} \alpha_{2,0}^{(j_1 j_2)} \left(\mathbf{g} + \Omega^{-1/2}\mathbf{w}\right) \mathcal{P}$$
$$- \frac{1}{3!} \Omega^{-1/2} \sum_{j_1=1}^{s} \sum_{j_2=1}^{s} \sum_{j_3=1}^{s} \frac{\partial^3}{\partial w_{j_1} \partial w_{j_2} \partial w_{j_3}} \alpha_{3,0}^{(j_1 j_2 j_3)}$$
$$\times \left(\mathbf{g} + \Omega^{-1/2}\mathbf{w}\right) \mathcal{P}$$
$$- \Omega^{-1/2} \sum_{j=1}^{s} \frac{\partial}{\partial w_j} \alpha_{1,1}^{(j)} \left(\mathbf{g} + \Omega^{-1/2}\mathbf{w}\right) \mathcal{P} + \mathcal{O}(\Omega^{-1}), \quad (22.89)$$

where $\mathbf{g}$ stands for $\mathbf{g}(\tau)$. From here, expansion of the quantities $\alpha_{km}^{(j_1 \cdots j_k)}(\mathbf{x})$ in powers of $\Omega^{-1/2}\mathbf{w}$ finally gives

$$\frac{\partial \mathcal{P}}{\partial \tau} - \Omega^{1/2} \sum_{j=1}^{s} \frac{dg_j}{d\tau} \frac{\partial \mathcal{P}}{\partial w_j} = -\Omega^{1/2} \sum_{j=1}^{s} \alpha_{1,0}^{(j)}(\mathbf{g}) \frac{\partial \mathcal{P}}{\partial w_j}$$
$$- \sum_{j=1}^{s} \sum_{k=1}^{s} \frac{\partial \alpha_{1,0}^{(j)}(\mathbf{g})}{\partial g_k} \frac{\partial}{\partial w_j} w_k \mathcal{P} + \frac{1}{2} \sum_{j_1=1}^{s} \sum_{j_2=1}^{s} \alpha_{2,0}^{(j_1 j_2)}$$
$$\times (\mathbf{g}) \frac{\partial^2 \mathcal{P}}{\partial w_{j_1} \partial w_{j_2}} + \mathcal{O}(\Omega^{-1/2}). \quad (22.90)$$

To avoid divergent terms in the limit $\Omega \to \infty$, we take $dg_j/d\tau = \alpha_{1,0}^{(j)}(\mathbf{g})$, $j = 1, \ldots, s$. In vector form, this is the same as letting $\mathbf{g}(\tau)$ be specified by

$$\frac{d\mathbf{g}}{d\tau} = \alpha_{1,0}(\mathbf{g}), \quad (22.91)$$

with the initial condition

$$\mathbf{g}(0) = \lim_{\Omega \to \infty} \frac{\mathbf{y}(0)}{\Omega}, \quad (22.92)$$

in consistency with Eq. (22.81); i.e., the initial state is determined with certainty and evolves deterministically through Eq. (22.91). Indeed Eq. (22.91) constitutes the deterministic, macroscopic evolution law. By keeping terms of order Ω^0 in Eq. (22.90), we obtain the Fokker–Planck equation:

$$\frac{\partial \mathcal{P}}{\partial \tau} = -\sum_{j=1}^{s} \sum_{k=1}^{s} \frac{\partial \alpha_{1,0}^{(j)}(\mathbf{g})}{\partial g_k} \frac{\partial}{\partial w_j} w_k \mathcal{P}$$
$$+ \frac{1}{2} \sum_{j_1=1}^{s} \sum_{j_2=1}^{s} \alpha_{2,0}^{(j_1 j_2)}(\mathbf{g}) \frac{\partial^2 \mathcal{P}}{\partial w_{j_1} \partial w_{j_2}}. \quad (22.93)$$

In chemical systems, we have the following identifications:

$$\tau = t, \quad (22.94)$$

$$\mathbf{g} = \lim_{\Omega \to \infty} \mathbf{N}/\Omega \equiv \mathbf{c} = (c_1, \ldots, c_s), \quad (22.95)$$

$$\mathbf{w} = \Omega^{-1/2}\mathbf{N} - \Omega^{1/2} \lim_{\Omega \to \infty} [\mathbf{N}/\Omega] = \Omega^{-1/2}\mathbf{N} - \Omega^{1/2}\mathbf{c}, \quad (22.96)$$

$$\alpha_{k0}^{(j_1 \cdots j_k)}(\mathbf{g}) = \lim_{\Omega \to \infty} \sum_{\rho} \nu_\rho^{j_1} \nu_\rho^{j_2} \ldots \nu_\rho^{j_k} k_\rho \prod_{i=1}^{s} \prod_{m=1}^{\nu_{\langle\rho}^{i}} \frac{N_i - m + 1}{\Omega}$$
$$= \sum_{\rho} k_\rho \nu_\rho^{j_1} \nu_\rho^{j_2} \ldots \nu_\rho^{j_k} \prod_{i=1}^{s} c_i^{\nu_{\langle\rho}^{i}} = \alpha_{k0}^{(j_1 \cdots j_k)}(\mathbf{c}), \quad (22.97)$$

$$\alpha_{km}^{(j_1 \ldots j_k)} = 0 \qquad (\text{if } m > 0). \quad (22.98)$$

Therefore, by making these replacements in Eq. (22.93), we obtain the multivariate Fokker–Planck equation for chemical systems with M reactions:

$$\frac{\partial \mathcal{P}(\mathbf{w}, t)}{\partial t} = \sum_{j=1}^{s} \sum_{k=1}^{s} \sum_{\rho=1}^{M} k_\rho \left[-\nu_\rho^j \frac{\partial \left(\prod_{i=1}^{s} c_i^{\nu_{<\rho}^{i}} \right)}{\partial c_k} \frac{\partial}{\partial w_j} (w_k \mathcal{P}) \right.$$
$$\left. + \frac{1}{2} \nu_\rho^j \nu_\rho^k \left(\prod_{i=1}^{s} c_i^{\nu_{<\rho}^{i}} \right) \frac{\partial^2 \mathcal{P}}{\partial w_j \partial w_k} \right], \quad (22.99)$$

where the concentrations c_i are time-dependent, their behavior being given by the macroscopic chemical kinetics Eq. (22.91) as

$$\frac{dc_j}{dt} = \sum_{\rho} k_\rho \nu_\rho^j \prod_{i=1}^{s} c_i^{\nu_{\langle\rho}^{i}} \qquad (j = 1, \ldots, s). \quad (22.100)$$

For example, for the Brusselator given by Eqs. (22.57)–(22.60), the macroscopic chemical kinetics given by the time evolution of the concentrations $c_X \equiv X/\Omega$ and $c_Y \equiv Y/\Omega$ of species X and Y is

$$\frac{dc_X}{dt} = k_1 - k_2 c_X + k_3 c_X^2 c_Y - k_4 c_X, \quad (22.101)$$

$$\frac{dc_Y}{dt} = k_2 c_X - k_3 c_X^2 c_Y. \quad (22.102)$$

Therefore, in the macroscopic limit $\Omega \to \infty$, we have $\mathbf{g} = \mathbf{y}/\Omega = (c_X, c_Y)$ from Eq. (22.81) and $\alpha_{1,0}(\mathbf{g}) = (k_1 -$

$k_2c_X + k_3c_X^2c_Y - k_4c_X, k_2c_X - k_3c_X^2c_Y$) from Eqs. (22.91), (22.101), and (22.102). By gathering all this information together with the stoichiometric numbers and numbers of reactants, the Fokker–Planck equation can then be written for the Brusselator, but we omit this here.

The general univariate Fokker–Planck equation is a particular instance of Eq. (22.93),

$$\frac{\partial \mathcal{P}(w,\tau)}{\partial \tau} = a(\tau)\frac{\partial (w\mathcal{P})}{\partial w} + b(\tau)\frac{\partial^2 \mathcal{P}}{\partial w^2} \tag{22.103}$$

with $a(\tau) \equiv -d\alpha_{1,0}(g)/dg$ and $b(\tau) \equiv \alpha_{2,0}(g)/2$. It can be explicitly solved for a Gaussian initial condition and boundary conditions $\mathcal{P}(\pm\infty,\tau) = 0$. Indeed, since

$$\mu(\tau) = \langle w(\tau)\rangle = \int_{-\infty}^{\infty} w\mathcal{P}(w,\tau)dw, \tag{22.104}$$

the Gaussian ansatz

$$\mathcal{P}(w,\tau) = \frac{1}{\sigma(\tau)\sqrt{2\pi}} e^{-\frac{(w-\mu(\tau))^2}{2\sigma(\tau)^2}} \tag{22.105}$$

allows the integration by parts of the equation

$$\begin{aligned}\frac{d\mu(\tau)}{d\tau} &= \int_{-\infty}^{\infty} w\frac{\partial \mathcal{P}(w,\tau)}{\partial \tau}dw \\ &= \int_{-\infty}^{\infty} w\left[a(\tau)\frac{\partial (w\mathcal{P})}{\partial w} + b(\tau)\frac{\partial^2 \mathcal{P}}{\partial w^2}\right]dw,\end{aligned} \tag{22.106}$$

where Eq. (22.103) has been used and the boundary conditions are to be applied. Thus, we obtain

$$\frac{d\mu(\tau)}{d\tau} = -a(\tau)\mu(\tau) \tag{22.107}$$

with solution

$$\mu(\tau) = \mu(0)e^{-\int_0^\tau a(t)dt}. \tag{22.108}$$

Since we also have

$$\sigma^2 = \left\langle w^2\right\rangle - \langle w\rangle^2 = \mu(\tau)^2 - \int_{-\infty}^{\infty} w^2\mathcal{P}(w,\tau)dw, \tag{22.109}$$

by taking the time derivative, replacing Eq. (22.103), integrating by parts over w, and applying the boundary conditions, we obtain

$$\frac{d\sigma(\tau)}{d\tau} = -a(\tau)\sigma(\tau) + \frac{b(\tau)}{\sigma(\tau)}, \tag{22.110}$$

which is readily solved as

$$\sigma(\tau) = e^{-\int_0^\tau a(t)dt}\sqrt{\sigma(0)^2 + 2\int_0^\tau dt' b(t')e^{2\int_0^{t'} a(t)dt}} \tag{22.111}$$

And, thus, by replacing Eqs. (22.108) and (22.111) in Eq. (22.105), one obtains the solution of the Fokker–Planck equation under the naturally imposed boundary conditions at infinity. The conclusion of the above analysis is that a probability distribution that is initially a Gaussian function of w keeps a Gaussian function at every later time. A simplest version of this univariate Fokker–Planck equation can be used, e.g., to provide an elegant description of Brownian motion [Risken, 1989].

Newton's equation of motion for a particle of mass m and velocity v_p in a medium with damping coefficient λ is given by

$$m\frac{dv_p}{dt} = -\lambda v_p. \tag{22.112}$$

This equation is readily integrated as $v_p(t) = v_p(0)e^{-\gamma t}$, where we have defined $\gamma \equiv \lambda/m$. If the mass of the particle is small enough, fluctuations on the velocity will be observed because of thermal agitation, and we shall have $m\left\langle v^2\right\rangle/2 = kT$ and, thus, a 'thermal velocity' $v_{th} \equiv \sqrt{\langle v^2\rangle} = \sqrt{2kT/m}$. We are then interested in finding the stochastic description of the dynamics of the particle. We can view $v_p(t)$ as the average (first moment) of a probability distribution $\mathcal{P}(v,t)$, and then from Eqs. (22.91), we can take $g = v_p$, $\tau = t$, and $\alpha_{1,0}(v_p) = -\gamma v_p$. Therefore, $a(\tau) = \gamma$ in Eq. (22.103). From equilibrium statistical mechanics, we know that the stationary probability distribution is the Maxwell distribution

$$\mathcal{P}_{\rm st}(v) = \lim_{\tau\to\infty}\mathcal{P}(v,t) = \sqrt{\frac{m}{2\pi kT}}e^{-\frac{mv^2}{2kT}}. \tag{22.113}$$

Therefore, by replacing Eq. (22.113) in Eq. (22.103), since $\partial P_{\rm st}/\partial t = 0$, we obtain $b(t) = \gamma kT/m$, and thus, the univariate Fokker–Planck equation that describes a Brownian particle is

$$\frac{\partial \mathcal{P}(v,t)}{\partial t} = \gamma\frac{\partial (v\mathcal{P})}{\partial v} + \frac{\gamma kT}{m}\frac{\partial^2 \mathcal{P}}{\partial v^2}. \tag{22.114}$$

One now gets, from Eqs. (22.108), (22.111), and (22.105), the time-dependent solution of Eq. (22.114) for any Gaussian initial condition and any time. If we, e.g., take a Dirac delta peaked at $v = v_p(0)$ as initial condition (and hence $\sigma(0) = 0$), we obtain

$$\mathcal{P}(v,t) = \frac{1}{\sigma(t)\sqrt{2\pi}}e^{-\frac{(v-\mu(t))^2}{2\sigma(t)^2}}, \tag{22.115}$$

$$\mu(t) = v_p(t) = v_p(0)e^{-\gamma t}, \tag{22.116}$$

$$\sigma(t) = \sqrt{\frac{kT}{m}}\left(1 - e^{-2\gamma t}\right) \tag{22.117}$$

at any other time t.

The Fokker–Planck equation has been used in the modeling of biomolecular motors [Schliwa, 2003,Bustamante et al.; 2001,Wang and Oster, 1998], in which irregularity in the motion of the motors arises as a consequence of molecular noise. In general, nonequilibrium fluctuations generated externally or by chemical reactions far from equilibrium can bias the Brownian motion of a particle in an anisotropic medium without thermal gradients [Astumian, 2001]. Such fluctuation-driven transport is one mechanism by which chemical energy can directly drive the motion of particles and macromolecules.

22.4.4 Numerical Simulation of the Chemical Master Equation: Gillespie's First Reaction Method

The chemical master equation, Eq. (22.55), cannot be analytically solved in general, and it usually poses daunting mathematical problems. However, useful numerical methods exist that are able to reproduce stochastic trajectories compatible with the chemical master equation. Most celebrated algorithms are due to Gillespie and are known as the 'Direct Method' and the 'First Reaction Method' [Gillespie, 1976, Gillespie, 1977]. In this section, we discuss the latter because it easily generalizes to time-dependent propensities, as shown in [Jansen, 1995]. (We discuss this generalization in Section 22.4.6.)

Let $P(\mathbf{N},t)$ denote the probability that, after a time t, a chemical system has been in the same state, with the number of particles $\mathbf{N}$ and no reaction taking place. This probability is provided by Eq. (22.67), with $\mathbf{y}=\mathbf{N}$ which, since the propensities do not depend on time, yields the result

$$P(\mathbf{N},t)=e^{-\sum_\rho W_\rho(\mathbf{N}+\nu_\rho|\mathbf{N})t}. \tag{22.118}$$

Let $P_\rho(\mathbf{N},t)$ denote the probability that, after a time t, reaction ρ has not occurred. Clearly, if there are M reactions in the network, we have

$$P(\mathbf{N},t)=\prod_{\rho=1}^{M}P_\rho(\mathbf{N},t), \tag{22.119}$$

where each $P_\rho(\mathbf{N},t)$ is given by

$$P_\rho(\mathbf{N},t)=e^{-W_\rho(\mathbf{N}+\nu_\rho|\mathbf{N})t}\qquad(\rho=1,\ldots,M). \tag{22.120}$$

Thus, those reactions for which the propensities are large are more likely to happen in a time interval τ, the probability $P_\rho(\mathbf{N},t)$ dropping to zero more strongly in those cases. By inverting Eq. (22.120), we can solve for the time τ_ρ that takes, at least, a reaction ρ to happen:

$$\tau_\rho=\frac{1}{W_\rho(\mathbf{N}+\nu_\rho|\mathbf{N})}\ln\left(\frac{1}{P_\rho}\right). \tag{22.121}$$

Therefore, those reactions with larger propensities and/or lower probability P_ρ not to happen, need a shorter time τ_ρ to happen.

Even when the probability $P(\mathbf{N},t)$ is different to the probability $p(\mathbf{N},t)$ entering the chemical master equation, the above development is fully compatible with the latter, because it is consistently based on the same behavior for the conditional probability density $p(\mathbf{N},t+\tau|\mathbf{N},t)$ as the chemical master equation.

The idea behind Gillespie's First Reaction Method is to use M equations (Eq. (22.121)) to generate M different times τ_ρ that are all obtained by drawing a random number P_ρ from the uniform distribution in the unit interval. Then the reaction with minimal τ_ρ is selected to advance. We give, for reference, Gillespie's algorithm in detail:

- Initialize the algorithm setting $t=0$ and $\mathbf{N}=\mathbf{N}_0$, and select a time $t_{\rm end}$ for the duration of the stochastic trajectory.
- Calculate all propensities $W_\rho(\mathbf{N}+\nu_\rho|\mathbf{N})$ from Eq. (22.56).
- Draw M different random numbers $P_\rho\in[0,1]$ $(\rho=1,\ldots,M)$ from the uniform distribution, and calculate M reaction times τ_ρ given by Eq. (22.121).
- Find $\mu\in[1,M]$ such that $\tau_\mu=\min\tau_\rho$, the reaction μ that has the shortest time to occur, in consistency with the random number generated. Select reaction μ to advance; i.e., put $\mathbf{N}\to\mathbf{N}+\nu_\mu$.
- If $t<t_{\rm end}$, put $t\to t+\tau_\mu$, and go to step 1; else, finish the algorithm.

We consider in the next section an application of this algorithm.

22.4.5 Application: Chemical Clocks at the Nanoscale

Chemical oscillations have been studied at the nanoscale, theoretically [Gaspard, 2002] and experimentally [McEwen et al., 2009, Visart de Bocarmé and Kruse, 2002]. The Brusselator is a well-known abstract model of a chemical clock, since it exhibits stable periodic dynamics in its macroscopic kinetics and has been considered to reach conclusions on the minimum number of particles that is able to sustain oscillations of reasonable quality [Gaspard, 2002]. We can investigate the impact of fluctuations on the oscillatory dynamics of the Brusselator by using Gillespie's First Reaction Method. In this way, we can obtain stochastic trajectories for the system when only a small number of molecules of species X and Y are present. These trajectories, as we have seen above, are fully compatible with the chemical master equation. Simulations can be run for different values of the system size Ω.

In the limit $\Omega\to\infty$, the dynamics of the Brusselator is given by Eqs. (22.101) and (22.102). From those equations, it is clear that there is a stationary, fixed point of the dynamics at $(X_{\rm st},Y_{\rm st})=(k_1/k_4,k_2k_4/(k_1k_3))$. This stationary state is stable for $k_2<k_{2,c}\equiv k_4+k_1^2k_3/k_4^2$. At $k=k_{2,c}$, the stationary state loses stability through a supercritical Hopf bifurcation to a stable limit cycle, which then develops in phase space for $k_2>k_{2,c}$ [Gaspard, 2002]. We consider next this limit cycle dynamics by taking the values $k_1=0.5$, $k_2=1.5$, $k_3=1$, and $k_4=1$ for the kinetic rate constants, so that we have $k_2>k_c=1.25$.

In Figure 22.3, simulations of the chemical master equation obtained by means of Gillespie's algorithm are shown. The leftmost column of panels in the figure corresponds to the macroscopic limit $\Omega\to\infty$, as obtained by numerically integrating Eqs. (22.101) and (22.102). The stochastic evolution of the Brusselator is shown for finite and decreasing values of the system size Ω. Shown in each case is the limit cycle in phase space (a) and the time evolution of

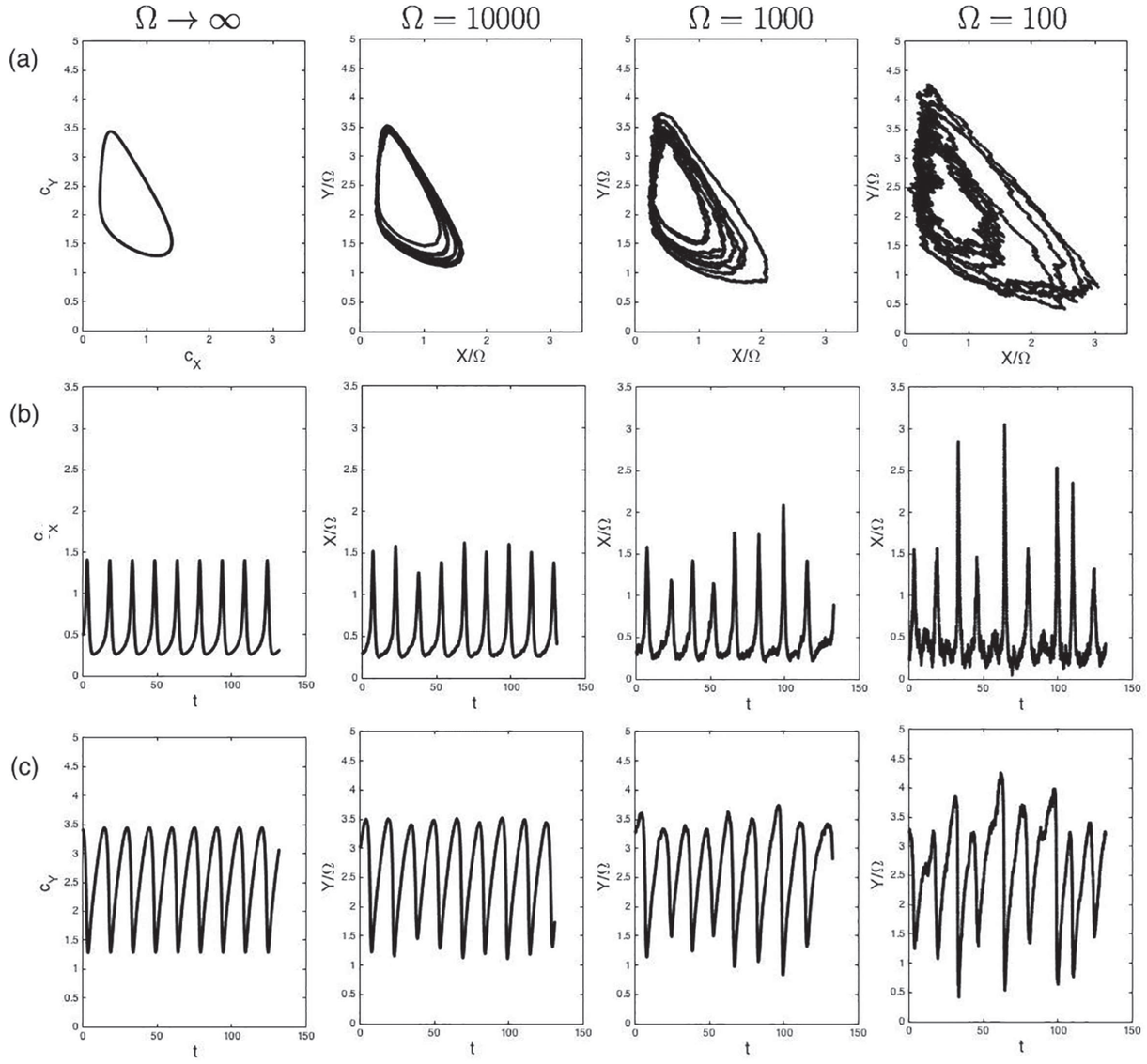

FIGURE 22.3 Phase space plots of the Brusselator dynamics obtained for the macroscopic limit $\Omega \to \infty$ (deterministic dynamics obtained integrating Eqs. (22.101) and (22.102)) and using Gillespie's algorithm with $\Omega = 10000$, $\Omega = 1000$, and $\Omega = 100$ as indicated over the panels. Shown is the limit cycle in phase space (a) and the temporal evolutions of X/Ω (b) and Y/Ω (c). In all panels, $k_1 = 0.5$, $k_2 = 1.5$, $k_3 = 1$, and $k_4 = 1$. The initial condition is in every panel the same $c_X(0) = X(0)/\Omega = 0.5$, $c_Y(0) = Y(0)/\Omega = 3.41$.

the concentrations $c_X = X/\Omega$ (b) and $c_Y = Y/\Omega$ (c). It is observed how the regular oscillations found in the macroscopic limit are affected by molecular fluctuations as the system size Ω is decreased. For $\Omega = 10000$, although apparent, the noise is weak enough so that the Fokker–Planck equation can be expected to provide a good description in this regime. However, as the system size is further decreased to $\Omega = 1000$, major deviations from regular oscillations are observed (even when their periodicity is kept), and for $\Omega = 100$, the limit cycle becomes very noisy, the oscillations being quite irregular. It can be shown that the autocorrelation function decays exponentially [Gaspard, 2002], and $\Omega = 100$ has been set as the approximate threshold below which the quality of chemical clocks is dramatically affected by molecular noise [Gaspard, 2002]. This highlights the fact that the nanoscale dynamics of chemical systems strongly departs from the macroscopic evolution laws owing to the stochastic events taking place and their discrete nature.

22.4.6 Generalized (Electro)Chemical Master Equation and the Extension of Gillespie's Algorithm

Electrochemical systems differ from chemical systems by the fact that the rate of an electrochemical reaction depends

on the electrode potential $\phi_{\rm dl}$. All information relevant to the macroscopic kinetics is provided by the Butler–Volmer electrochemical equations, which express this relationship through a preexponential factor which is analogous to the chemical rate constant and an exponential dependence on the electrode potential [Bard and Faulkner, 2004]. On a nanoelectrode, the stochastic nature of electrochemical reactions has to be considered. The problem is, however, more complex, since, in addition to the number of chemical species, there may be electron transfer to/from the electrode, and the electrode potential can become a fluctuating variable as well [García-Morales and Krischer, 2010].

In this section, we discuss the electrochemical master equation, which extends the chemical master equation to account for the effect of the stochastic variable $\phi_{\rm dl}$ on the system dynamics. Therefore, we consider an extended state for the system as given now by a vector $\mathcal{N} = (\phi_{\rm dl}, N_1, \ldots, N_s)$, where the electrode potential ϕ is incorporated to the 'chemical part' ruling the numbers of particles of the s different chemical species $\mathbf{N} = (N_1, \ldots, N_s)$. Therefore, Eq. (22.54) of a chemical system extends to

$$\sum_{i=1}^{s} \nu^i_{<\rho} N_i + n_{<\rho} e^- \xrightarrow{k_\rho(\phi_{\rm dl})} \sum_{i=1}^{s} \nu^i_{>\rho} N_i + n_{>\rho} e^- \quad (22.122)$$

for an electrochemical system. The number of electrons transferred is a new feature compared to chemical systems and is given by $n_\rho = n_{>\rho} - n_{<\rho}$. Again, the stoichiometric numbers $\nu^i_\rho = \nu^i_{>\rho} - \nu^i_{<\rho}$ control the number of molecules of each species formed or consumed each time the reaction takes place. In the following, we shall denote by $\widetilde{\nu}_\rho = (n_\rho, \nu^1_\rho, \ldots, \nu^s_\rho)$ the vector of stoichiometric coefficients $\nu_\rho = (\nu^1_\rho, \ldots, \nu^s_\rho)$, typical of chemical systems, extended by the number of electrons transferred, n_ρ.

The macroscopic rate of electron transfer $k^{(\rm mac)}_\rho$ depends on the electrode potential, $\phi_{\rm dl}$, at which the electron transfer takes place in the following form (Butler–Volmer kinetics):

$$k^{(\rm mac)}_\rho(\phi_{\rm dl}) = k^0_\rho e^{c_\rho(\phi_{\rm dl} - \phi^0_{\rm dl})}. \quad (22.123)$$

Here $\phi^0_{\rm dl}$ is the redox potential of the reaction; the preexponential factor k^0_ρ does not depend on the electrode potential and $c_\rho = \frac{(\beta_\rho - \alpha)|n_\rho|F}{RT}$ where $\beta_\rho = 0$ for reduction reactions and 1 for oxidation reactions, α is the transfer coefficient, F the Faraday constant, R the ideal gas constant, and T the temperature [García-Morales and Krischer, 2010].

A typical electrochemical experiment is controlled by applying an external voltage U between the working and the reference electrodes [Krischer, 2003]. For nanoscale electrodes, an ohmic resistance R_e (e.g., a lipid molecule anchored to a conductive macroscopic support) is often introduced as spacer linking the nanoelectrode (e.g., a metallic nanoparticle) to the external control. Any such arrangement renders the electrode potential $\phi_{\rm dl}$ a dynamic variable of the system. The evolution of $\phi_{\rm dl}$ is dictated by charge conservation at the interface. The total current flowing through the system I splits into two components, a capacitive one $I_{\rm cap}$ involved in the charging of the double layer and a faradaic one I_F coming from electrochemical reactions involving electron transfer to/from the electrode. Charge conservation at the interface implies $I_{\rm cap} = I - I_F$ or equivalently

$$C\frac{d\phi_{\rm dl}}{dt} = -i_F(\phi_{\rm dl}) + \frac{U - \phi_{\rm dl}}{R_e A}, \quad (22.124)$$

where C is the double layer capacitance per surface area, $A = a_0\Omega$ is the area of the electrode, with a_0 denoting the density of surface sites, and $i_F = I_F/A$. Between two times, $t_0 = t$ and $t + \tau$, where no reaction event takes place at the nanoelectrode, the faradaic current is zero, the above equation can be analytically solved, yielding

$$\phi_{\rm dl}(t + \tau) = U + (\phi_{\rm dl}(t) - U)e^{-\frac{\tau}{R_e C A}}. \quad (22.125)$$

Let τ_ρ be the time after which a stochastic reaction event occurs, reaction ρ taking place. Then, a number n_ρ of electrons are transferred and make a contribution to the Faradaic current. Therefore, Eq. (22.125) takes the form

$$\phi_{\rm dl}(t + \tau_\rho) = U + (\phi_{\rm dl}(t) - U)e^{-\frac{\tau_\rho}{R_e C A}} - \frac{n_\rho e}{CA}. \quad (22.126)$$

For times $\tau_\rho << R_e CA$, this equation can be approximated by

$$\phi_{\rm dl}(t + \tau_\rho) = \phi_{\rm dl}(t) + \frac{U - \phi_{\rm dl}(t)}{R_e CA}\tau_\rho - \frac{n_\rho e}{CA}. \quad (22.127)$$

The validity of this approximation needs to be checked for very small nanoelectrodes. The stochastic dynamics of the electrochemical system is thus given by a master equation, where the propensities are explicitly dependent on time,

$$\frac{\partial p(\mathcal{N}, t)}{\partial t} = \sum_\rho \left[W_\rho(\mathcal{N}|\mathcal{N} - \widetilde{\nu}_\rho, t)p(\mathcal{N} - \widetilde{\nu}_\rho, t) - W_\rho(\mathcal{N} + \widetilde{\nu}_\rho|\mathcal{N}, t)p(\mathcal{N}, t)\right], \quad (22.128)$$

since they are given by

$$W_\rho(\mathcal{N} + \widetilde{\nu}_\rho|\mathcal{N}, t) = e^{c_\rho \phi_{\rm dl}} W_\rho(\mathbf{N} + \nu_\rho|\mathbf{N}) = e^{c_\rho(\phi_{\rm dl} - \phi^0_{\rm dl})}\Omega k^0_\rho \prod_{i=1}^{s}\prod_{m=1}^{\nu^i_{\langle\rho}} \frac{N_i - m + 1}{\Omega}, \quad (22.129)$$

which explicitly depend on time through $\phi_{\rm dl}(t)$, whose evolution we shall assume as being provided by Eq. (22.127).

Let $P(\mathcal{N}, t)$ denote the probability that, after a time t, an electrochemical system has been in the same state, with vector $\mathcal{N}$, no reaction taking place. Following the approach suggested in [Jansen, 1995, Koper et al., 1998], we can generalize Gillespie's algorithm, calculating the appropriate expressions for the waiting times of each reaction ρ to occur. In order to do this, we must take into account that the propensities now depend on time through the double layer potential. From Eq. (22.67), we now have

$$P(\mathcal{N},\tau_\rho)=\exp\left(-\sum_\rho\int_t^{t+\tau_\rho}W_\rho(\mathcal{N}+\widetilde{\mu}_\rho|\mathcal{N},t')dt'\right), \tag{22.130}$$

and the probability that reaction ρ has not occurred is given by

$$\begin{aligned}P_\rho(\mathcal{N},\tau_\rho)&=\exp\left(-\int_t^{t+\tau_\rho}W_\rho(\mathcal{N}+\widetilde{\mu}_\rho|\mathcal{N},t')dt'\right)\\&=\exp\left(-W_\rho(\mathbf{N}+\nu_\rho|\mathbf{N})\int_t^{t+\tau_\rho}\exp\left[c_\rho\phi_{\rm dl}(t')\right]dt'\right)\\&=\exp\left(-W_\rho(\mathbf{N}+\nu_\rho|\mathbf{N})\int_t^{t+\tau_\rho}\exp\left[c_\rho\phi_{\rm dl}(t)\right.\right.\\&\quad\left.\left.+\frac{U-\phi_{\rm dl}(t)}{R_eCA}c_\rho(t'-t)\right]dt'\right)\\&=\exp\left(-\frac{\exp\left[c_\rho\phi_{\rm dl}(t)\right]W_\rho(\mathbf{N}+\nu_\rho|\mathbf{N})R_eCA}{c_\rho\left(U-\phi_{\rm dl}(t)\right)}\right.\\&\quad\left.\times\left[\exp\left(\frac{U-\phi_{\rm dl}(t)}{R_eCA}c_\rho\tau_\rho\right)-1\right]\right),\end{aligned} \tag{22.131}$$

which can be inverted to give

$$\begin{aligned}\tau_\rho=&\frac{R_eCA}{c_\rho(U-\phi_{\rm dl}(t))}\ln\\&\times\left[1+\frac{c_\rho(U-\phi_{\rm dl}(t))}{\exp\left[c_\rho\phi_{\rm dl}(t)\right]W_\rho(\mathbf{N}+\nu_\rho|\mathbf{N})R_eCA}\ln\left(\frac{1}{P_\rho}\right)\right],\end{aligned} \tag{22.132}$$

where P_ρ is a number drawn from the uniform probability distribution. When there are no electron transfer reactions involved, $c_\rho=0$, and by applying L'Hopital's rule to Eq. (22.132), we find the waiting time of a purely chemical system, Eq. (22.121):

$$\tau_\rho=\frac{1}{W_\rho(\mathbf{N}+\nu_\rho|\mathbf{N})}\ln\left(\frac{1}{P_\rho}\right). \tag{22.133}$$

The extension of Gillespie's algorithm to simulate the evolution of the electrochemical master equation now proceeds as follows:

- Initialize the algorithm setting $t=0$ and $\mathcal{N}=\mathcal{N}_0$, and select a time t_{end} for the duration of the stochastic trajectory.
- Calculate all propensities $W_\rho(\mathcal{N}+\widetilde{\nu}_\rho|\mathcal{N})$ from Eq. (22.129).
- Draw M different random numbers P_ρ ($\rho=1,\ldots,M$) from the uniform distribution, and calculate M positive reaction times τ_ρ given by Eq. (22.132)
- Find $\mu\in[1,M]$ such that $\tau_\mu=\min\tau_\rho$. The reaction μ has the shortest time to occur, in consistency with the random number generated. Select reaction μ to advance, i.e., put $\mathcal{N}\to\mathcal{N}+\widetilde{\nu}_\mu$, the potential being updated by means of Eq. (22.127).
- If $t<t_{end}$, put $t\to t+\tau_\mu$ and go to step 1; else, finish the algorithm.

This algorithm has allowed to simulate electrochemical systems at the nanoscale from elementary reaction steps [García-Morales and Krischer, 2010, García-Morales and Krischer, 2011] to more complex reaction networks as the reduction of H_2O_2 on a Pt electrode [Mukouyama et al., 2001, García-Morales and Krischer, 2010], a reaction that is known to display oscillations at the macroscale [Mukouyama et al., 2001]. Because of fluctuations on the double layer potential $\phi_{\rm dl}$, electrochemical reaction steps occur faster at the nanoscale than at the macroscale [García-Morales and Krischer, 2010, García-Morales and Krischer, 2011]. Quite interestingly, the distribution of the double layer potential shows asymmetries [García-Morales and Krischer, 2011, García-Morales and Krischer, 2011] which have been related to Tsallis spectral statistics [Tsekouras and Tsallis, 2005] and superstatistics [Beck and Cohen, 2003, Beck and Cohen, 2004]. Indeed, it has been found that the stochastic kinetics of nanoscale electrochemical systems can be described by a superstatistical framework with an averaged Tsallis-like entropic parameter $q_{\rm av}$ that measures the impact of nanoscale correlations caused by the double layer potential and which is given by [García-Morales and Krischer, 2011]

$$q_{\rm av}=1-\frac{c_\rho(U-\langle\phi_{\rm dl}\rangle)}{R_eCA\left\langle W_\rho(\mathbf{N}+\nu_\rho|\mathbf{N})\right\rangle}, \tag{22.134}$$

where the brackets in Eq. (22.134) denote time averages along a stochastic trajectory. We note that for a macroscopic electrode, $A\to\infty$ and $q_{\rm av}\to1$ so that Boltzmann–Gibbs thermostatistics is regained. However, at the nanoscale, A can be small enough so that, in general, $0\leq q_{\rm av}\leq1$. This additional role of the stochastic double layer potential in electrochemical systems makes nanoscale electrochemical clocks less robust to molecular noise than purely chemical clocks [Cosi and Krischer, 2017]. Indeed, electrode sizes on the scale of 100–500 $\rm nm^2$ are likely to be needed in order to observe time-correlated oscillations [Cosi and Krischer, 2017]. Note, however, that the low-noise regime of chemical and electrochemical systems display similar features: the propensities in the electrochemical master equation have the canonical form given by Eq. (22.78) in van Kampen's expansion, and a rigorous Fokker–Planck for electrochemical systems can be derived, matching the general expression Eq. (22.93). Thus, in contrast to other treatments that employ the Langevin equation in the weak noise limit [Gabrielli et al.; 1993,Keizer, 1987], the approach presented in [García-Morales and Krischer, 2010] together with van Kampen's expansion of the master equation, here discussed, is able to rigorously describe the behavior of electrochemical systems from the macroscale to the nanoscale, even in regimes where noise is strong and a small number of particles are present.

22.5 Summary and Conclusions

The significant advances in the field of nanothermodynamics over the past decades have been summarized, with special

attention to the foundations of nonequilibrium nanothermodynamics from stochastic processes.

The size-dependent thermodynamic properties in mono- and multicomponent systems associated with the surface energy contributions have attracted considerable attention since the late nineteenth century. Although the field is rather mature, many interesting results are still being achieved, thanks to the advances in the experimental techniques.

Hill's nanothermodynamics has proved to be successful in many fields, including the description of metastable states and complex relaxation kinetics. We have focused here on its equilibrium statistical thermodynamics basis. In the recent developments of this theory by Chamberlins group, the interactions between the nanosystems have been satisfactorily described using a mean-field approach in combination with completely open nanosystems that are allowed to adjust their size.

The range of applications of Tsallis nonextensive thermostatistics has proved to be extremely broad. This theory has been presented here as a thermodynamic formalism that can be used to study nanosystems, especially in the presence of correlations. It has been connected to the theory of superstatistics and to the fluctuations in the Boltzmann parameter.

The master equation constitutes a general and powerful tool for the stochastic modeling of nonequilibrium nanosystems beyond the linear branch of nonequilibrium thermodynamics. This equation allows the Fokker–Planck equation to be rigorously derived in the weak noise limit and, thus, it also provides an understanding on how macroscopic deterministic dynamics emerges out of an inherently probabilistic description. Although the nonlinear effects cause couplings in the collective dynamics, rigorous results of general validity can be established. These results include the integral FTs, which are of enormous interest for the understanding of both equilibrium and nonequilibrium processes at the nanoscale.

Acknowledgements

J. C. and J. A. M. thank financial support from Ministerio de Ciencia, Innovación y Universidades and the European Regional Development Funds through project PGC2018-097359-B-100.

References

Abe, S. and Okamoto, Y. 2001. *Nonextensive Statistical Mechanics and its Applications.* Berlin: Springer.

Ali, S.; Myasnichenko, V. S. and Neyts, E. C. 2016. Size-dependent strain and surface energies of gold nanoclusters. *Phys. Chem. Chem. Phys.* 18: 792–800.

Alloyeau, D.; Prevot, G.; Le Bouar, Y.; Oikawa, T.; Langlois, C.; Loiseau, A. and Ricolleau, C. 2010. Ostwald ripening in nanoalloys: When thermodynamics drives a size-dependent particle composition. *Phys. Rev. Lett.* 105: 255901.

Astumian, R. D. 2001. Thermodynamics and kinetics of a Brownian motor. *Science* 276:917–22.

Bard, A. and Faulkner, L. 2004. *Electrochemical Methods.* New York: Wiley.

Beck, C. 2002. Non-additivity of Tsallis entropies and fluctuations of temperature. *Europhys. Lett.* 57: 329–33.

Beck, C. and Cohen, E. G. D. 2003. Superstatistics. *Physica A* 322:267–75.

Beck, C. and Cohen, E. G. D. 2004. Superstatistical generalization of the work fluctuation theorem. *Physica A* 344:393–402.

Brandao, F.; Horodecki, M.; Ngc, N.; Oppenheim, J. and Wehner S. 2015. The second laws of quantum thermodynamics. *Proc. Natl. Acad. Sci.* 112: 3275–9.

Brites, C. D. S.; Lima, P. P.; Silva, N. J. O.; Mill, A.; Amaral, V. S.; Palacio, F. and Carlos, L. D. 2012. Thermometry at the nanoscale. *Nanoscale* 4:4799–829.

Bustamante, C.; Keller, D. and Oster, G. 2001. The physics of molecular motors. *Acc. Chem. Res.* 34:412–20.

Cartwright, J. 2014. Roll over, Boltzmann. Does Tsallis entropy really add up? *Phys. World* 27: 31–5.

Castelvecchi, D. 2017. Clash of the physics laws. *Nature* 543:597–8.

Chamberlin, R. V. 2015. The big world of nanothermodynamics. *Entropy* 17: 52–73.

Chandler, D. 1987. *Introduction to Modern Statistical Mechanics.* New York: Oxford University.

Chen, C. L.; Lee, J.-G.; Arakawa, K. and Mori, H. 2011. Quantitative analysis on size dependence of eutectic temperature of alloy nanoparticles in the Ag-Pb system. *Appl. Phys. Lett.* 98: 083108.

Chushak, Y. G. and Bartell, L. S. 2001. Melting and freezing of gold nanoclusters. *J. Phys. Chem. B* 105: 11605-14.

Cosi, F. G. and Krischer, K. 2017. Destructive impact of molecular noise on nanoscale electrochemical oscillators. *Eur. Phys. J. Spec. Top.* 226:1997–2013.

Couchman, P. R. and Jesser, W. A. 1977. Thermodynamic theory of size dependence of melting temperature in metals. *Nature* 269: 481–3.

Crooks, G. E. 1999. Entropy production fluctuation theorem and the nonequilibrium work relation for free-energy differences. *Phys. Rev. E* 60: 2721–6.

Defay, R. and Prigogine I. 1966. *Surface Tension and Adsorption.* London: Longmans.

DeHoff, R. 2006. *Thermodynamics in Materials Science.* Boca Raton, FL: Taylor & Francis.

Evans, D. J.; Cohen, E. G. D. and Morriss G. P. 1993. Probability of second law violations in shearing steady states. *Phys. Rev. Lett.* 71:2401.

Evans, D. J. and Searles, D. J. 1994. Equilibrium microstates which generate second law violating steady states. *Phys. Rev. E* 50:1645–1648.

Evans, D. J. and Searles, D. J. 1992. The fluctuation theorem. *Adv. Phys.* 51:1529–1585

Evans, D. J.; Searles, D. J. and Williams, S. R. 2016. *Fundamentals of Classical Statistical Thermodynamics.*

Dissipation, Relaxation, and Fluctuation Theorems. Weinheim: Wiley.

Falcioni, M.; Villamaina, D.; Vulpiani, A.; Puglisi, A. and Sarracino, A. 2011. Estimate of temperature and its uncertainty in small systems. *Am. J. Phys.* 19: 777–85, 19: 980.

Farrell, H. H. and Van Siclen, C. D. 2007. Binding energy, vapor pressure, and melting point of semiconductor nanoparticles. *J. Vac. Sci. Technol. B.* 71:1441-7.

Ford, I. 2013. *Statistical Physics. An Entropic Approach.* Chichester: Wiley.

Gabrielli, C.; Huet, F.; and Keddam, M. 1993. Fluctuations in electrochemical systems. I. General theory on diffusion limited electrochemical reactions. *J. Chem. Phys.* 99:7232–9.

García-Morales, V.; Cervera, J. and Pellicer, J. 2004. Coupling theory for counterion distributions based in Tsallis statistics. *Physica A* 339:482–90.

García-Morales, V.; Cervera, J. and Pellicer, J. 2005. Correct thermodynamic forces in Tsallis thermodynamics: Connection with Hill nanothermodynamics. *Phys. Lett. A* 336:82–8.

García-Morales, V. and Pellicer, J. 2006. Microcanonical foundation of nonextensivity and generalized thermostatistics based on the fractality of the phase space. *Physica A* 361:161–72.

García-Morales, V. and Krischer, K. 2010. Fluctuation enhanced electrochemical reaction rates at the nanoscale. *Proc. Nat. Acad. Sci.* 107:4528–32.

García-Morales, V.; Cervera, J. and Manzanares, J. A. 2011. Nanothermodynamics. In K. D. Sattler (ed.) *Handbook of Nanophysics. Principles and Methods*, ch.15. Boca Raton, FL: CRC Press.

García-Morales, V. and Krischer, K. 2011. Superstatistics in nanoscale electrochemical systems. *Proc. Nat. Acad. Sci.* 108:19535–9.

García-Morales, V. and Krischer, K. 2011. Kinetic enhancement in nanoscale electrochemical systems caused by non-normal distributions of the electrode potential. *J. Chem. Phys.* 134:244512.

Gardiner, N. G. 2009. *Stochastic Methods: A Handbook for the Natural and Social Sciences.* New York: Springer.

Gaspard, P. 2002. The correlation time of mesoscopic chemical clocks. *J. Chem. Phys.* 117:8905–16.

Gheorghiu, S. and Coppens, M. O. 2004. Heterogeneity explains features of "anomalous" thermodynamics and statistics. *Proc. Natl. Acad. Sci. USA* 101: 15852-6.

Gillespie, D. T. 1976. A general method for numerically simulating the stochastic time evolution of coupled chemical reactions. *J. Comput. Phys.* 22:403–34.

Gillespie, D. T. 1977. Exact stochastic simulation of coupled chemical reactions. *J. Phys. Chem.* 81:2340–61.

Haag, G. 2017. *Modelling with the Master Equation: Solution Methods and Applications in Social and Natural Sciences.* Cham: Springer.

Hill, T.L. 1994. *Thermodynamics of Small Systems.* New York: Dover.

Hill, T.L. 2001. A different approach to nanothermodynamics. *Nano Lett.* 1:273–5.

Hill, T. L. and Chamberlin, R.V. 2002. Fluctuations in energy in completely open small systems. *Nano Lett.* 2: 609–13.

Horodecki, M. and Oppenheim, J. 2013. Fundamental limitations for quantum and nanoscale thermodynamics. *Nature Comm.* 4:2059.

Inzoli, I.; Kjelstrup, S.; Bedeaux, D. and Simon, J. M. 2010. Thermodynamic properties of a liquid-vapor interface in a two-component system. *Chem. Engn. Sci.* 65: 4105–16.

Jabbareh, M. A. and Monji F. 2018. Thermodynamic modeling of Ag-Cu nanoalloy phase diagram. *Calphad* 60: 208–13.

Jansen, A. 1995. Monte Carlo simulations of chemical reactions on a surface with time-dependent reaction rate constants. *Comput. Phys. Commun.* 86:1–12.

Jiang, Q. and Wen, Z. 2011. *Thermodynamics of Materials.* Berlin: Springer.

Kaszkur, Z. 2013. Thermodynamical properties of nanoalloys. In F. Calvo (ed.) *Nanoalloys. From Fundamentals to Emergent Applications*, chap. 5. Amsterdam: Elsevier.

Keizer, J. 1987. *Statistical Thermodynamics of Nonequilibrium Processes.* New York: Springer.

Kondepudi, D. 2008. *Introduction to Modern Thermodynamics.* New York: Wiley.

Kofman, R.; Cheyssac, P.; Lereah, Y. and Stella, A. 1999. Melting of clusters approaching 0D. *Eur. Phys. J. D* 9: 141–4.

Koper, M.; Jansen, A.; van Santen, R.; Lukkien, J.; and Hilbers, P. 1998. Monte Carlo simulations of a simple model for the electrocatalytic Co oxidation on platinum. *J. Chem. Phys.* 109:6051–62.

Krischer, K. 2003. Nonlinear dynamics in electrochemical systems. In Kolb, D. M. and Alkire, R. C. (eds.) *Advances in Electrochemical Sciences and Engineering*, Vol. 8, pp.89-208. Weinheim: Wiley.

Kurchan, J. 1998. Fluctuation theorem for stochastic dynamics. *J. Phys. A Math. Gen.* 31:3719–29.

Lebowitz J. L. and Spohn, H. 1999. A Gallavotti-Cohen-type symmetry in the large deviation functional for stochastic dynamics. *J. Stat. Phys.* 95: 333-65.

Li, Z. H. and Truhlar, D. G. 2014. Nanothermodynamics of metal nanoparticles. *Chem. Sci.* 5: 2605–24.

Lu, H. M. and Jiang, Q. 2005. Size-dependent surface tension and Tolmans length of droplets. *Langmuir* 21:779-81.

McEwen, J. S.; Gaspard, P.; Visart de Bocarmé, T.; and Kruse, N. 2009. Nanometric chemical clocks. *Proc. Nat. Acad. Sci.* 106:3006–10.

Mafé, S.; Manzanares, J. A. and de la Rubia, J. 2000. On the use of the statistical definition of entropy to justify Plancks form of the third law of thermodynamics. *Am. J. Phys.* 68: 932–5.

Mahler, G. 2015. *Quantum Thermodynamics Processes: Energy and Information Flows at the Nanoscale.* New York: Pan Stanford.

Manzanares, J. A.; Peljo, P. and Girault, H. H. 2017. Understanding digestive ripening of ligand-stabilized, charged metal nanoparticles. *J. Phys. Chem. C* 121: 13405-11.

Mukouyama, Y.; Nakanishi, S.; Chiba, T.; Murakoshi, K. and Nakato, Y. 2001. Mechanisms of two electrochemical oscillations of different types, observed for h_2o_2 reduction on a Pt electrode in the presence of a small amount of halide ions. *J. Phys. Chem. B.* 105:7246–53.

Nanda, K. K.; Maisels, A.; Kruis, F. E.; Fissan, H. and Stappert, S. 2003. Higher surface energy of free nanoparticles. *Phys. Rev. Lett.* 91: 106102.

Naudts, J. 2011. *Generalised Thermostatistics.* Springer: London.

Nicolis, G.. 1972. Fluctuations around nonequilibrium states in open nonlinear systems. *J. Stat. Phys.* 6:195–222.

Nicolis, G. and Prigogine, I. 1977. *Self-Organization in Nonequilibrium Systems.* New York: Wiley.

Oppenheim, I.; Schuler, K. E. and Weiss, G. H. 1977. *Stochastic Processes in Chemical Physics: The Master Equation.* Cambridge: The MIT Press.

Park, J. and Lee, J. 2008. Phase diagram reassessment of Ag–Au system including size effect. *Calphad* 23: 135–41.

Peljo, P.; Manzanares, J. A. and Girault, H. H. 2016. Contact potentials, Fermi level equilibration, and surface charging. *Langmuir* 32:5765–75.

Peljo, P.; Manzanares, J. A. and Girault, H. H. 2017. Variation of the Fermi level and the electrostatic force of a metallic nanoparticle upon colliding with an electrode. *Chem. Sci.* 8: 4795–803, 8: 5206.

Peters, K. F.; Cohen, J. B. and Chung, Y. W. 1998. Melting of Pb nanocrystals. *Phys. Rev. B* 57: 13430–8.

Pohl, J.; Stahl, C. and Albe, K. 2012. Size-dependent diagrams of metallic alloys: A Monte Carlo simulation study on order-disorder transitions in Pt-Rh nanoparticles. *Beilstein J. Nanotechnol.* 3:1–11.

Risken, H. 1989. *The Fokker–Planck Equation: Methods of Solution and Applications.* New York: Springer.

Scanlon, M. D.; Peljo, P.; Mndez, M. A.; Smirnov, E. and H. H. Girault 2015. Charging and discharging at the nanoscale: Fermi level equilibration of metallic nanoparticles. *Chem. Sci.* 6: 2705–20.

Schliwa, M. 2003. *Molecular Motors.* Weinheim: Wiley.

Schmelzer J. W. P.; Boltachev, G. Sh. and Abyzov, A. S. 2013. Temperature of critical clusters in nucleation theory: Generalized Gibbs' approach. *J. Chem. Phys.* 139: 034702.

Seifert, U. 2005. Entropy production along a stochastic trajectory and an integral fluctuation theorem. *Phys. Rev. Lett.* 95:040602.

Seifert, U. 2012) Stochastic thermodynamics, fluctuation theorems and molecular machines. *Rep. Prog. Phys.* 75:126001.

Sevick, E. M.; Prabhakar, R.; Williams, S. R. and Searles, D. J. 2008. Fluctuation theorems. *Annu. Rev. Phys. Chem.* 59:603-33.

Shi, Z.; Wynblatt, P. and Srinivasan, S. G. 2004. Melting behaviour of nanosized lead particles embedded in an aluminium matrix. *Acta Mater.* 52: 2305–16.

Spinney, R. and Ford, I. 2013. Fluctuation relations: A pedagogical overview. In R. Klages, W. Just and C. Jarzynski (eds.) *Nonequilibrium Statistical Physics of Small Systems. Fluctuation Relations and Beyond*, chap. 1. Weinheim: Wiley.

Sugimoto, T. and Shiba, F. 1999. A new approach to interfacial energy. 3. Formulation of the absolute value of the solid-liquid interfacial energy and experimental collation to silver halide systems. *J. Phys. Chem. B* 103: 3607–15.

Tsallis, C. 1988. Possible generalization of Boltzmann-Gibbs statistics. *J. Stat. Phys.* 52:479–87.

Tsallis, C. 2005. Is the entropy S_q extensive or nonextensive? In C. Beck, G. Benedek, A. Rapisarda, and C. Tsallis (eds.) *Complexity, Metastability and Nonextensivity. 31st Workshop of the International School of Solid State Physics*, pp. 13–32. Singapore: World Scientific.

Tsallis, C. 2009. *Introduction to Nonextensive Statistical Mechanics. Approaching a Complex World.* New York: Springer.

Tsekouras, G. A.; and Tsallis, C. 2005. Generalized entropy arising from a distribution of q indices. *Phys. Rev. E* 71:046144.

van Kampen, N. G. 2007. *Stochastic Processes in Physics and Chemistry.* Amsterdam: North Holland (Elsevier).

Visart de Bocarmé, T. and Kruse, N. 2002. Kinetic instabilities during the NO(x) reduction with hydrogen on Pt crystals studied with field emission on the nanoscale. *Chaos* 12:118-30.

Wang, H. and Oster, G. 1998. Energy transduction in the F1 motor of ATP synthase. *Nature (London)* 396: 279–282.

Wang, C. X.; Yang, Y. H.; Xu, N. S. and Yang, G. W. 2004. Thermodynamics of diamond nucleation on the nanoscale. *J. Am. Chem. Soc.* 126: 11303–6.

Wang, C. X. and Yang, G. W. 2005. Thermodynamics of metastable phase nucleation at the nanoscale. *Mat. Sci. Engn. R* 49: 157–202.

Yang, C. C. and Li, S. 2008. Size-dependent temperature-pressure phase diagram of carbon. *J. Phys. Chem. C* 112: 1423–6.

Zhang, C. Y.; Wang, C. X.; Yang, Y. H. and Yang, G. W. 2004. A nanoscaled thermodynamic approach in nucleation of CVD diamond on nondiamond surfaces. *J. Phys. Chem. B* 108: 2589-93.